Cretaceous Research 78 (2017) 34–55

Contents lists available at ScienceDirect

Cretaceous Research

journal homepage: www.elsevier.com/locate/CretRes

Litho- and biostratigraphy, facies patterns and depositional sequences of the Cenomanian-Turonian deposits in the Ksour Mountains (Saharan Atlas, Algeria)

Madani Benyoucef [a, *], Kaddour Mebarki [b], Bruno Ferré [c], Mohammed Adaci [b], Luc Georges Bulot [d, e], Delphine Desmares [f], Loïc Villier [f], Mustapha Bensalah [b], Camille Frau [g], Christina Ifrim [h], Fatima-Zohra Malti [i]

[a] Faculté des Sciences de la Nature et de la Vie, Université de Mascara, 29000 Mascara, Algeria
[b] Département des Sciences de la Terre et de l'Univers et Laboratoire de Recherche n°25, Université Abou-Bekr Belkaid, Tlemcen, Algeria
[c] Dame du Lac 213, 3 rue Henri Barbusse, F-76300 Sotteville-lès-Rouen, France
[d] UM 34 Cerege CNRS (UMR 7630) – IRD (UMR 161), Aix-Marseille Université (Centre Saint-Charles), Place Victor Hugo, 13331 Marseille Cedex 03, France
[e] NARG, University of Manchester, School of Earth Atmospheric and Environmental Sciences, Williamson Building, Oxford Road, Manchester M13 9PL, United Kingdom
[f] Université Paris VI, UMR 7207 CR2P "Paléobiodiversité et Paléoenvironnements" 4 place Jussieu, 75252 Paris Cedex 05, France
[g] Groupement d'Intérêt Paléontologique, Science et Exposition, 60 bd Georges Richard, 83000 Toulon, France
[h] Institut für Geowissenschaften, Ruprecht-Karls-Universität, Im Neuenheimer Feld 234, 69120 Heidelberg, Germany
[i] Université de Béchar, PB.417 Béchar, Algeria

ARTICLE INFO

Article history:
Received 3 November 2016
Accepted in revised form 9 May 2017
Available online 11 May 2017

Keywords:
Cenomanian-Turonian
Saharan Atlas
Stratigraphy
Facies analysis
Depositional environments
Sequential evolution

ABSTRACT

The Cenomanian-Turonian deposits exposed in the Ksour Mountains, western part of the Saharan Atlas (Algeria), document marine shelf environments that had been thriving on the North African passive margin, connected northwards to the Tethys Ocean, and fringed southwards by the Saharan craton. Their lithological, palaeontological, and sedimentological characteristics have been investigated to provide new insights into the biostratigraphy, palaeo-environmental evolution and sea-level changes in this western part of the Saharan Atlas. Three formations are recognized, from base to top of the studied succession: 1. The El Rhelida Formation comprising two informal units: the mixed siliciclastic-carbonate unit deposited under different flow regime conditions, from shoreline to backshore environments, and the limestone–claystone unit including coastal mudflat deposits prone to storm events. The early Cenomanian age of the El Rhelida Formation is supported by vertebrate assemblages. 2. The Mdaouer Formation comprising two units: the evaporitic unit dominated by claystone and evaporite alternations deposited on a flat coastal sabkha with occasional storms, and the marlstone–limestone unit formed in a peritidal-lagoonal environment. The Mdaouer Formation is of early-middle Cenomanian age. 3. The Rhoundjaïa Formation comprising three units: the lower limestone unit consisting of relatively homogeneous fossiliferous limestones; the middle marly unit composed of marlstone and bioclastic limestones, and the upper limestone unit consisting of carbonates showing vertical variations in faunal content and stratonomy. The Rhoundjaïa Formation was deposited in homoclinal ramp setting. Ammonite data indicate an early late Cenomanian to early Turonian age for this interval. Within an overall transgressive trend, the Cenomanian-Turonian deposits of the Ksour Mountains record three third-order depositional sequences bounded each by regional discontinuities.

1. Introduction

The Cretaceous deposits are widely distributed in Northern Africa along the southern margin of the former Tethys Ocean. On the Algerian territory, the Cretaceous exposures are well-known and

* Corresponding author.
E-mail address: benyoucefmada@gmail.com (M. Benyoucef).

http://dx.doi.org/10.1016/j.cretres.2017.05.013
0195-6671/

have been mapped repeatedly over the past 60 years, particularly those of South Algeria, in the Saharan Atlas and the Sahara, which from west to east links the Moroccan-Algerian, the Tunisian and the Libyan-Algerian basins. Only a few recent studies addressed the Upper Cretaceous litho-, biostratigraphy, and sedimentological evolution of the South Algeria (Grosheny et al., 2008 and Chikhi-Aouimeur et al., 2011 for the eastern part of the Saharan Atlas; Benyoucef and Meister, 2015 and Benyoucef et al., 2016 for the Guir Basin; and Amédro et al., 1996; Busson et al., 1999; Grosheny et al., 2013; Zaoui et al., 2016 and Ferré et al., 2016 for the Tinrhert Basin). Apart from Mebarki et al. (2016) and Ferré et al. (2017), no geological work have been recently carried out on the Ksour Mountains, since the 1970s, the lithostratigraphic studies of the Upper Cretaceous succession are generally scarce and only available in unpublished thesis (e.g., Flamand, 1911; Cornet, 1952; Galmier, 1970; Bassoullet, 1973; Douihasni, 1976).

Here, we describe the Cenomanian-Turonian formations exposed in the Ksour Mountains in order to clarify their stratigraphy. We provide new data about the ichnological and palaeontological content of the studied formations, and new biostratigraphic ages derived from fossil vertebrates, ammonites, ostracodes and foraminifers. Additionally, we present the first detailed description for the lower Upper Cretaceous sedimentary record of the western Saharan Atlas. The depositional environments are interpreted from the facies description, and sequential scheme. The lithostratigraphic terminology follows Bassoullet (1973).

2. Geographical and geological setting

The Saharan Atlas domain (or Atlas system), forming the core of the present study, is a poorly deformed intra-continental system, extending some 1,200 km along a SW-NE direction, from the eastern end of the Moroccan High Atlas to the western part of the Tunisian Atlas. To the north, this belt is juxtaposed to a tabular domain of the High Plateaus (the so-called Eastern Meseta or Oran Meseta), the southern boundary of the Saharan Atlas is represented by a major tectonic break, termed the Sahara Flexure (Laffite, 1939) or South Atlas Fault (SAF), the Saharan Atlas is juxtaposed to the Saharan Platform. The Saharan Atlas (also called Pre-Saharan Atlas) includes a series of subranges: the Ksour Mountains connected to the Moroccan High Atlas in the west, the Djebel Amour in the middle, and the Ouled-Naïl Mountains, the Aurès Mountains, the Hodna Mountains and the Nememcha-Mzab Mountains in its eastern part (Fig. 1A).

The study area is located in the Ksour Mountains that occupied the western part of the Saharan Atlas. The core of this inverted-rift structure belt consists of a Palaeozoic metamorphic basement. The overlying sedimentary cover comprises marine and continental deposits of Mesozoic and Cenozoic age. The Triassic deposits are mainly represented by minor outcrops displaying a red-bed facies, such as shales with evaporites (Ain Ouarka diapir). These Upper Triassic evaporites are also locally associated with basaltic flows, probably related to the initial rifting of the Atlantic Ocean (Ambroggi, 1963). During the Early-Middle Jurassic, marine

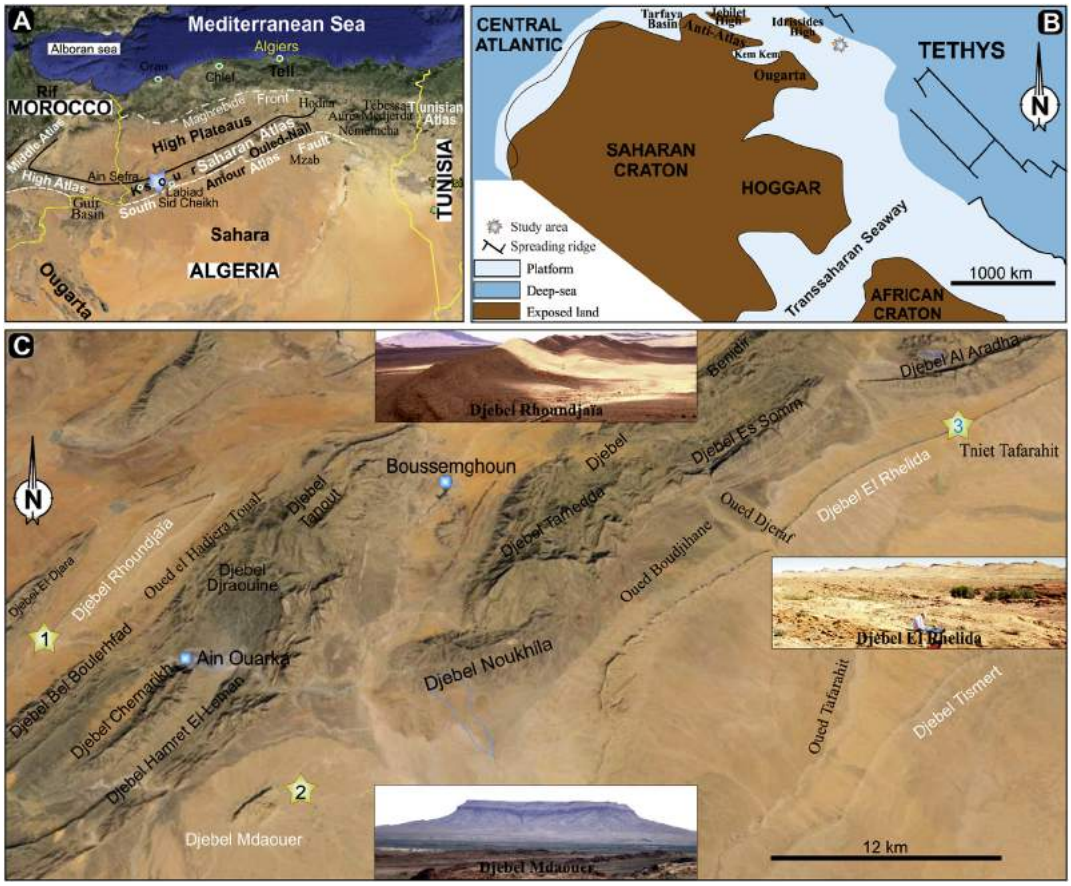

Fig. 1. Palaeogeographic and geographic framework of the study area. A, Satellite image of the study area (from Google earth); B, Palaeogeographic position of the Saharan Atlas at the Cenomanian-Turonian times (palaeogeographic map after Blakey, 2011). C, Photographs and satellite location (from Google earth) of the three studied sections.

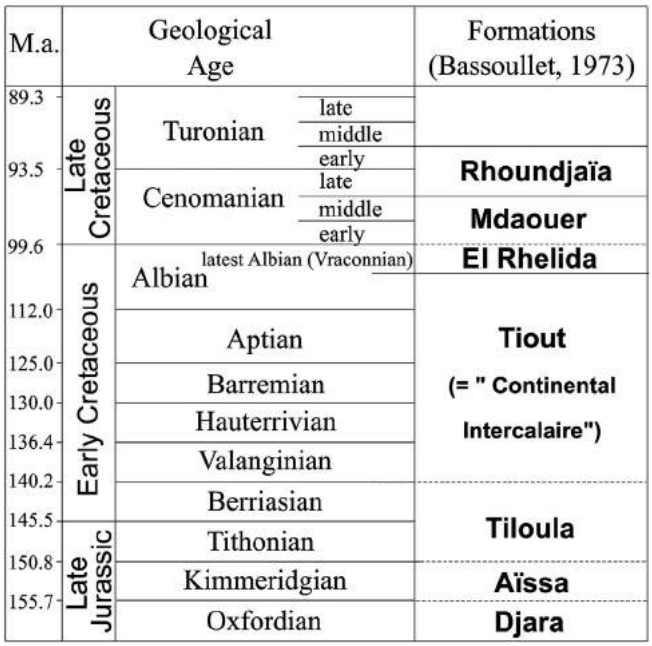

Fig. 2. Stratigraphic nomenclature for the Upper Jurassic-Cretaceous series of the Ksour Mountains (numerical ages taken from a Geologic Time Scale 2013).

conditions had been prevailing and the Ksour basin was then filled in with thick limestone-dominated deposits. These latter are overlain by a ca 3,000 m-thick series of Upper Jurassic-Lower Cretaceous siliciclastic, mostly continental, deposits ranging from Oxfordian to latest Albian in age (Fig. 2; Bassoullet, 1973). By the end of the Albian, or at the beginning of the Cenomanian, existed a wide range of sedimentary environments that registered event beds similar to those already evidenced in the neighbouring Saharan Platform. During the early Late Cretaceous, the Saharan Atlas was part of a large shallow epi-continental sea, at the southern margin of the oceanic Tethys, between the Tello-Mesetan domain to the north and the African shield to the south. The lower Upper Cretaceous sediments mainly document a marine platform setting that developed on the North African passive margin, connected to the Tethys Ocean to the North, and bordered by the Saharan craton uplands to the South (Fig. 1B). In the Ksour Mountains, they form three lithostratigraphic units, from base to top: (1) the mixed siliciclastic-carbonates of the El Rhelida Formation; (2) the marlstone-evaporite deposits of the Mdaouer Formation; and (3) the limestones–marlstones of the Rhoundjaïa Formation (Figs. 2–4).

During the Eocene and the Oligocene, the Mesozoic succession had been uplifted and folded (Dewey et al., 1973); the Cenomanian-Turonian succession is superbly exposed along several valleys (e.g., Oued Namous, Oued El Hadjera Toual and Oued Boudjihane) in the flanks of anticlines. The limestone ledge usually occupies the top of perched synclines (e.g., Djebel Mdaouer; Djebel Rhoundjaïa; Djebel El Rhelida and Djebel Tismert) (Fig. 1C).

3. Methodology

The investigation of three outcrops, between the cities of Ain Sefra and Labiad Sid Cheikh, (Fig. 1A and C), allowed us to build a composite section (Fig. 4). Some 125 rock samples were collected and more than 40 thin sections were processed for microfacies analysis. The most representative succession (Section 3 in Fig. 1; coordinates UMTS: 31S 244171 E; 3635433 N) stretches in the valley between Djebel El Rhelida and Oued Boudjihane. Section 2 (coordinates UMTS: 30S 775485 E; 3616610 N) is located in Djebel Mdaouer, 40 km west of the El Rhelida section, in the same area as the section described by Bassoullet (1973). In our section, the El Rhelida and the Mdaouer formations are well exposed. The lower and middle parts of the Rhoundjaïa Formation are better exposed here than in the Djebel El Rhelida section. Approximately 20 km north of the Djebel Mdaouer section, situated on the westernmost part of Djebel Rhoundjaïa, at Section 1 (coordinates UMTS: 30S 759177 E; 3627043 N), only the Rhoundjaïa Formation outcropping in good condition shows the same characteristics as that of Djebel Mdaouer. Lateral changes are observed in the Rhoundjaïa Formation where the middle marly unit changes its thickness eastwards in Section 3. The thickest marlstone interval (middle marly unit, see below) can be observed in sections 1 and 2.

All available sedimentological and palaeontological data were considered in interpretation of the depositional environments. Palaeontological analyses are qualitative.

Fig. 3. General view of the Cenomanian-Turonian strata in the Ksour Mountains (Oued Boudjihane-Djebel El Rhelida section). 1 – upper part of the Tiout Formation ("Continental intercalaire"), 2 – El Rhelida Formation, 3 – Mdaouer Formation, 4 – Rhoundjaïa Formation.

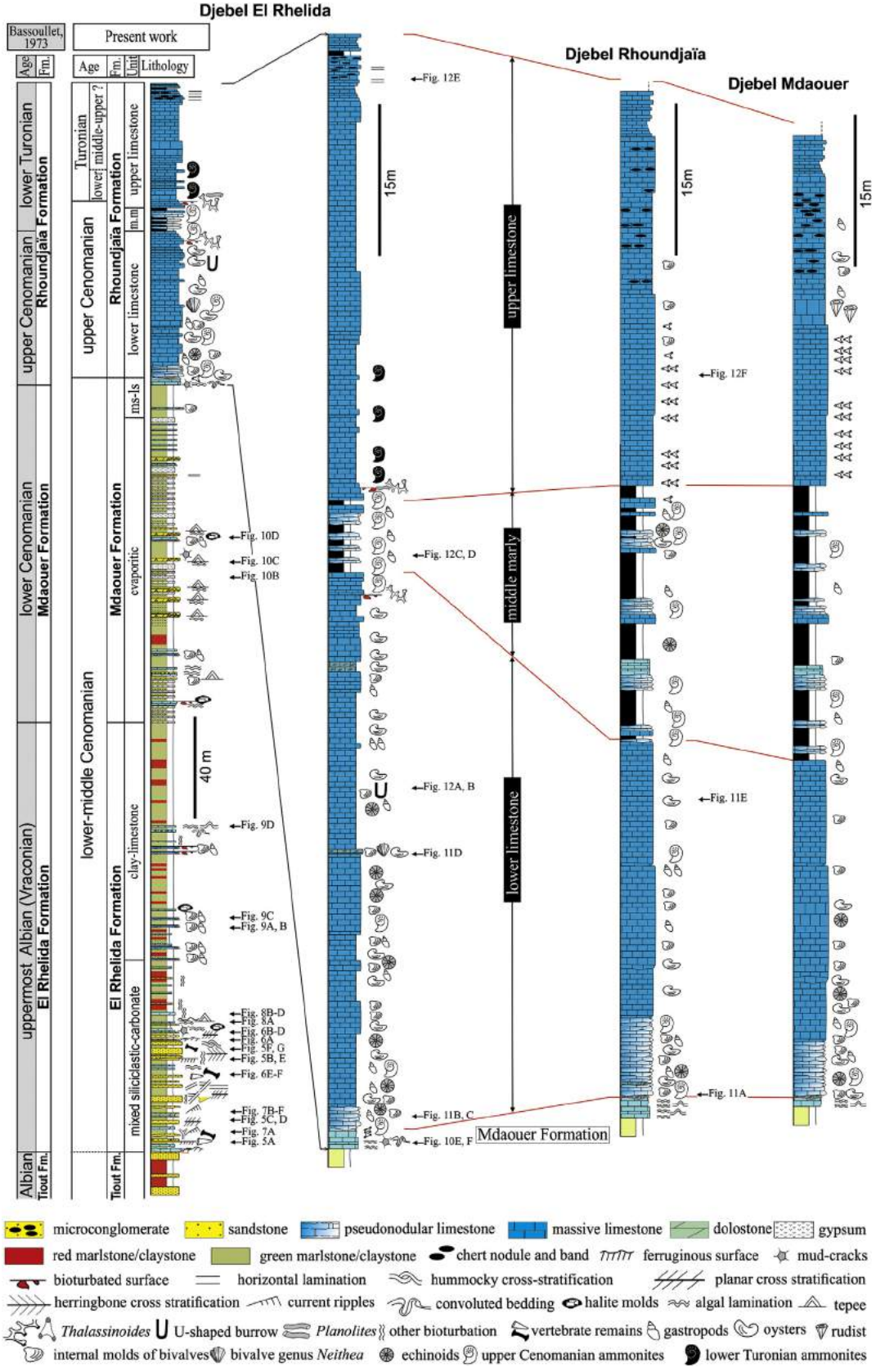

Fig. 4. Stratigraphic succession of the Cenomanian-Turonian in the Ksour Mountains.

4. Lithostratigraphic framework

The first stratigraphic synthesis and nomenclature of the Mesozoic deposits in the Ksour Mountains was introduced by Bassoullet (1973): the sedimentary succession overlying the Lower Cretaceous Tiout Formation, referred to as the upper part of the "Continental intercalaire" group, can be classified into three main lithostratigraphic formations: The El Rhelida Formation (Vraconnian = uppermost Albian), the Mdaouer Formation (lower Cenomanian) and the Rhoundjaïa Formation (upper Cenomanian-lower Turonian). These formations are revised hereafter and described in details below, from older to younger (Figs. 2–4).

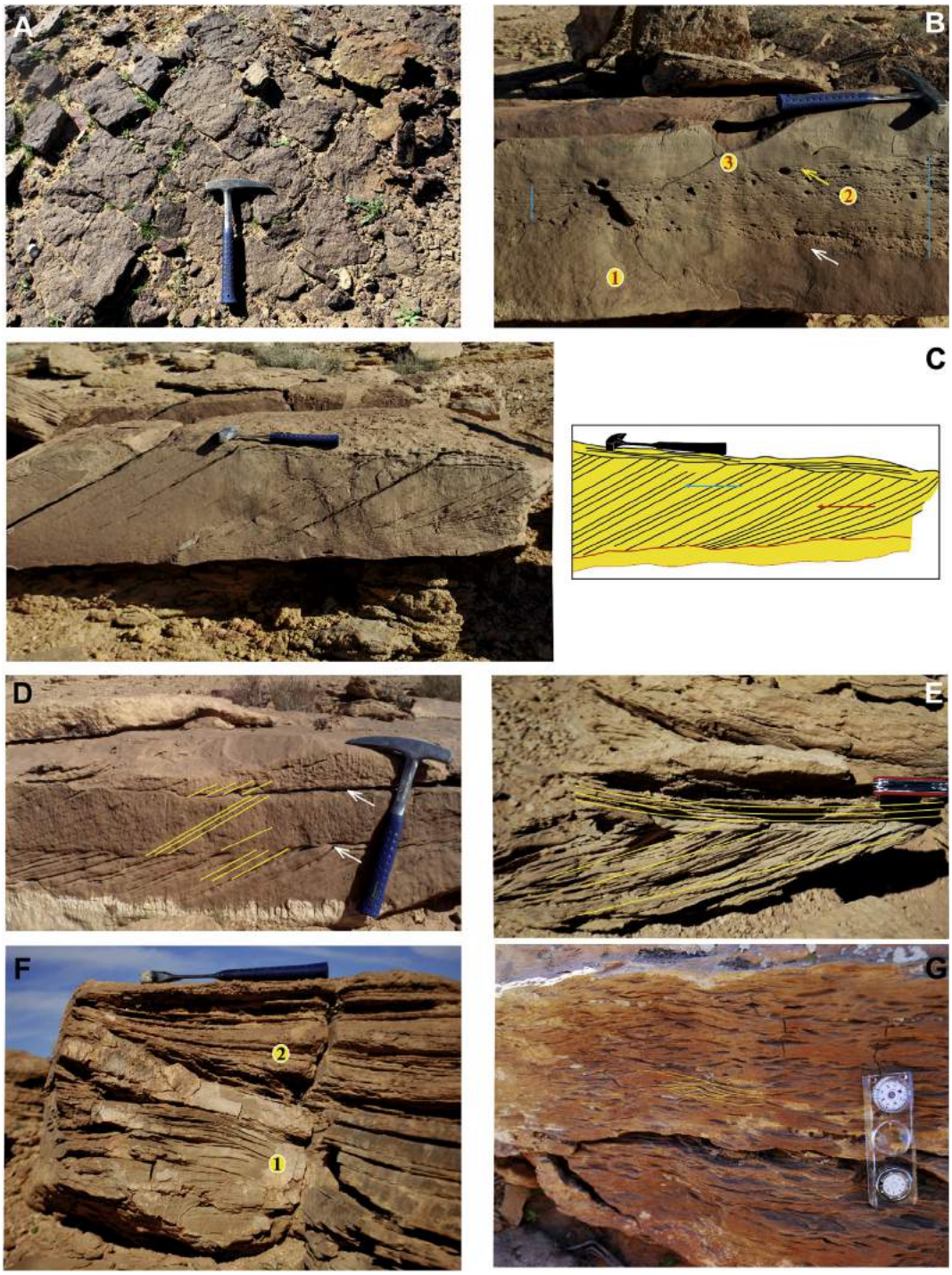

Fig. 5. Sedimentary structures of the siliciclastic facies framing the lower unit of the El Rhelida Formation. A, Oxidized sandstone bed in the mixed siliciclastic-carbonate unit (Oued Boudjihane area); B, A set of planar cross-strata truncated by a planar erosion surface. The erosion surface (marked by arrow) is draped by a set of thin climbing ripple laminae (vertical bars) that follows the morphology of the erosion surface; C, Sandstone bed presenting the transition from tangential oblique stratification to oblique angular structure (red arrow: strong current, blue arrow: low current); D, Sandstone bed presenting planar cross stratification interrupted by reactivation surfaces (arrow); E, Sandstone showing trough-cross stratification; F, Sandstone presenting hummocky cross-stratification (1) overlain by a set of low angle planar stratification (2); G, Sandstone showing wavy cross-bedding. (For interpretation of the references to colour in this figure legend, the reader is referred to the web version of this article.)

4.1. El Rhelida Formation

The reference section of the El Rhelida Formation was originally coined by Bassoullet (1973) in Djebel El Rhelida (Fig. 1C). Its thickness varies from 150 m at Djebel Mdaouer to 160 m in Djebel El Rhelida, and is poorly exposed in Djebel Rhoundjaïa. It directly overlies the Lower Cretaceous Tiout Formation and underlies the Mdaouer Formation. Its base is defined at the first limestone bed capping the fully siliciclastic Tiout Formation. This bed is hard, 20–30 cm thick, undulating, violet (Oued Boudjihane area) to rust-coloured (Oued Ladjraf area) and shows linguoid ripple marks covered by a ferruginous crust at their top surface. The upper boundary of the formation coincides with the appearance of the first gypsum bed that defines the base of the Mdaouer Formation.

Above the basal limestone bed, the El Rhelida Formation is dominated by sand deposits turning upwards into clay–limestone, allowing the distinction of two informal units:

4.1.1. Mixed siliciclasticcarbonate unit

This lower unit is well developed in the valley of Oued Boudjihane on the northern foot of Djebel El Rhelida. It represents a transitional zone between the Tiout clastic Formation (= "Continental intercalaire") and the clay–limestone alternations of the second unit (herein called the "upper El Rhelida" unit). It is composed mainly of sandstones and red or green clays (about 75% of the total thickness of the unit) which alternate with repetitive intercalations of limestones and occasionally oxidized sandstones (Fig. 5A) and microconglomeratic deposits. The sandstones are frequently overlain by limestone beds. They form tabular units, up to 1 m thick, with 10–80 cm-thick beds showing sharp or slightly erosional bases, occasionally channelized. A wide variety of sedimentary structures (ripple cross-lamination, hummocky cross-lamination, wave ripple cross-lamination, planar and herringbone cross-stratification) characterize these sandstones that, for descriptive purposes, can be arranged into six facies (Fig. 5B–G, Fig. 6A–B, see also FT3 to FT7 in Table 1). The top surface of some sandstone levels also shows wave current ripples and sinuous bifurcating ripples (Fig. 6C–D), ferruginous crusts and synaeresis cracks.

The micro-conglomeratic levels (Fig. 6E–F) are rare, intercalated in sandstones and mainly composed of sub-rounded clasts, usually centimetric in diameter and variable in lithology, embedded in a

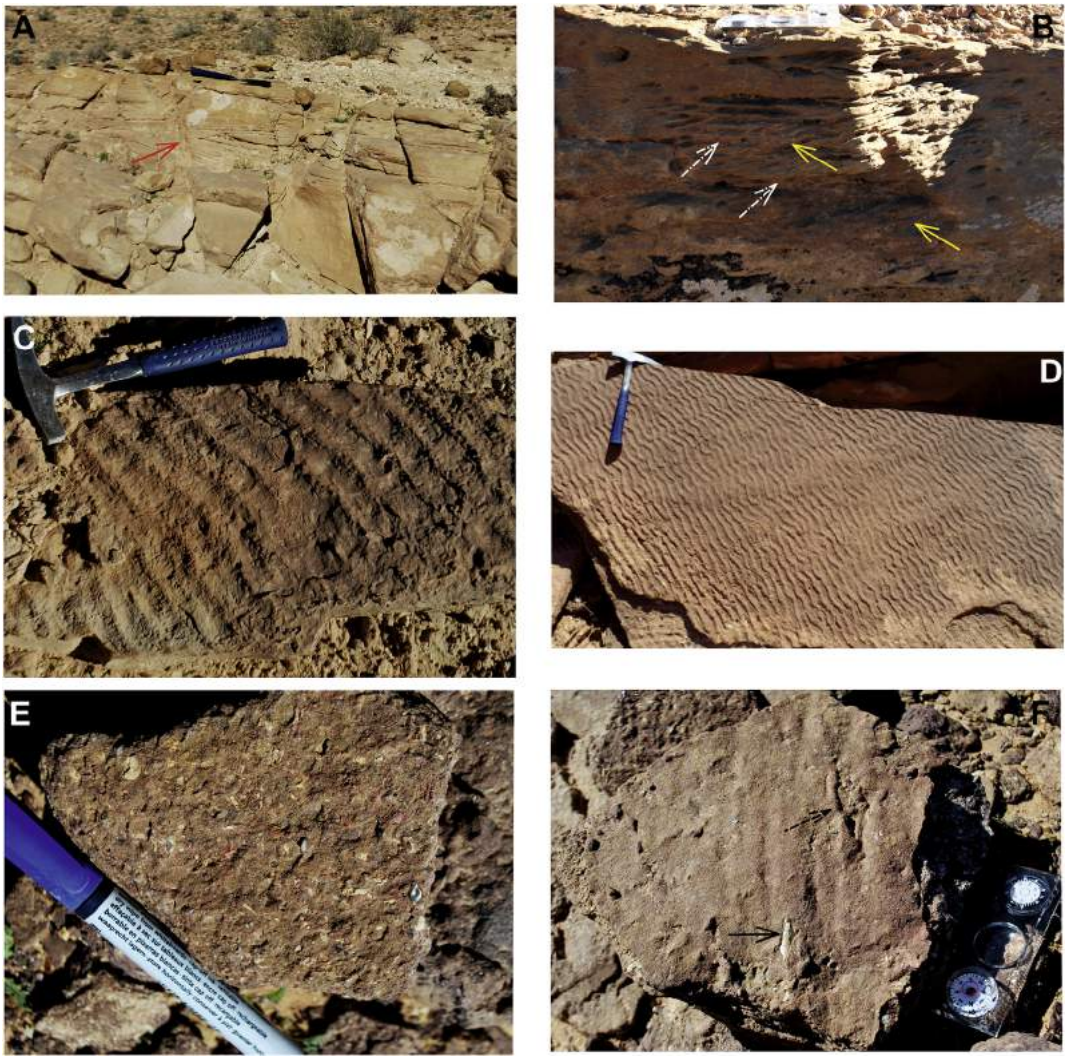

Fig. 6. Field photographs of the siliciclastic facies building the lower unit of El Rhelida Formation. A, Hummocky cross-lamination (arrow) in sandstone bed at the base of El Rhelida Formation; B, Sandstone showing climbing ripple laminae (continuous arrow) truncated by reactivation surfaces (broken arrow); C, Symmetrical wave ripples on the top surface of a sandstone bed; D, Fine-grained sandstone bed in the vicinity of the Oued Boudjihane showing symmetrical wave-generated ripples (ripple profiles are symmetrical and crests bifurcate); E, Micro-conglomeratic bed containing shark remains and bone debris; F, Isolated tooth of *Spinosaurus aegyptiacus* (continuous arrow) and indeterminate burrow (discontinuous arrow) at the top surface of a conglomeratic bed.

brownish sandstone matrix. They range from 5 to 15 cm in thickness, are laterally discontinuous and contain a heterogeneous variety of phosphatic particles, fish debris, unspecified shark remains and bone debris, turtle plates, cm-sized isolated teeth of *Spinosaurus aegyptiacus* Stromer, *Spinosaurus* sp., ganoid scales of *Lepidotes* sp., fragmentary bones of *Mawsonia* sp. and *Neoceratodus africanus* Haug, isolated teeth of pycnodontiform fishes, and rostral fragments of *Onchopristis numidus* (Haug). The top surfaces of some micro-conglomerate layers show ripple marks and indeterminate burrows (Fig. 6F).

Strongly bioturbated, fine- to medium grained sandstone beds are showing in the middle part of the unit. Ichnofossils *Bergaueria*, *Helminthopsis*, *Lockeia*, *Planolites* cf. *beverleyensis*, *Planolites montanus*, *Rhabdoglyphus*, *Spirophycus*, and *Thalassinoides* were identified (Fig. 7). These massive bioturbated sandstones bodies are laterally continuous over several tens of metres, range from 10 to 30 cm in thickness, and are devoid of any primary sedimentary structures or faunal content.

The carbonate beds, 10–40 cm thick, are represented by bio-laminated mudstones (Fig. 8A), massive dolostones (Fig. 8B) with birdseye and fenestrae fabrics and evaporite pseudo-morphs. The top surface of beds shows usually asymmetric and linguoid current ripples (Fig. 8C), mud-cracks and perforations in pairs attributed to ichnogenus *Diplocraterion* (Fig. 8D).

4.1.2. Clay–limestone unit

This upper unit comprises green and red clay irregularly alternating with yellow to cream massive bioclastic limestones, ranging from 5 to 25 cm in thickness, extending laterally over several hundred metres, and containing abundant remains of bivalves (e.g., *Pseudoptera anomala* Sowerby, Fig. 9A), gastropods and unspecified ostracodes. Some bioclastic beds show a deformed horizontal

Fig. 7. Representative field photographs of bioturbation in the mixed siliciclastic-carbonate unit (scale bar: 1 cm, ruler: 9 cm). A, Intensively bioturbated sandstone including horizontal network of *Thalassinoides*; B, Lower surface of a sandstone bed with circular to slightly sub-circular bulbs of *Bergaueria* (1) and dark-coloured tunnels of cf. *Planolites montanus* (2); C, Lower surface of sandstone bed including round imprints with high positive hyporelief attributed to ichnogenus *Bergaueria* (1) and large horizontal tunnels of *Planolites beheileyensis* (2); D, Bedding planes of a fine-grained sandstone displaying irregularly meandering, unbranched, horizontal burrows of ichnogenus *Helminthopsis* (1) and round imprints with convex hyporelief of ichnogenus *Bergaueria* (2); E, Well-preserved trace fossil as positive relief on the sole of a sandstone bed with spiral pattern corresponding to ichnogenus *Spirophycus* (1) and straight strings and narrow cylinders of varying length encircled at regular or irregular intervals by ring-like "knots" or well-defined swellings that display no bifurcation referable to ichnogenus *Rhabdoglyphus* (2); F, *Bergaueria* (1) and *Rhabdoglyphus* (2) trace fossils associated to small oblong horizontal bodies pointed at both ends preserved as convex hypo-relief assigned to ichnogenus *Lockeia* (3).

Fig. 8. Outcrop pictures of the carbonate facies from the lower unit of El Rhelida Formation. A, Bio-laminated mudstone; B, Massive dolostone. Note the irregular lower surface of the bed; C, Symmetrical ripple marks at the top of a limestone; D, Top surface of a thin dolostone bed with fossilized *Diplocraterion* burrows.

network of *Thalassinoides* burrows (Fig. 9B) and horizontal branched burrows of *Ophiomorpha* (Fig. 9C) at their basal surface. Their top surface displays current ripples. The green claystone can also be intercalated by thin bio-laminated limestone levels barren of any fauna but sometimes containing dewatering structures (Fig. 9D) and halite moulds.

4.2. Mdaouer Formation

The reference section of the Mdaouer Formation was originally located by Bassoullet (1973) around Djebel Mdaouer (from Mdaouer: isolated and of circular form, in Arabic language, Fig. 1C). Its thickness varies from 120 m in Djebel Mdaouer to 130 m in Djebel El Rhelida.

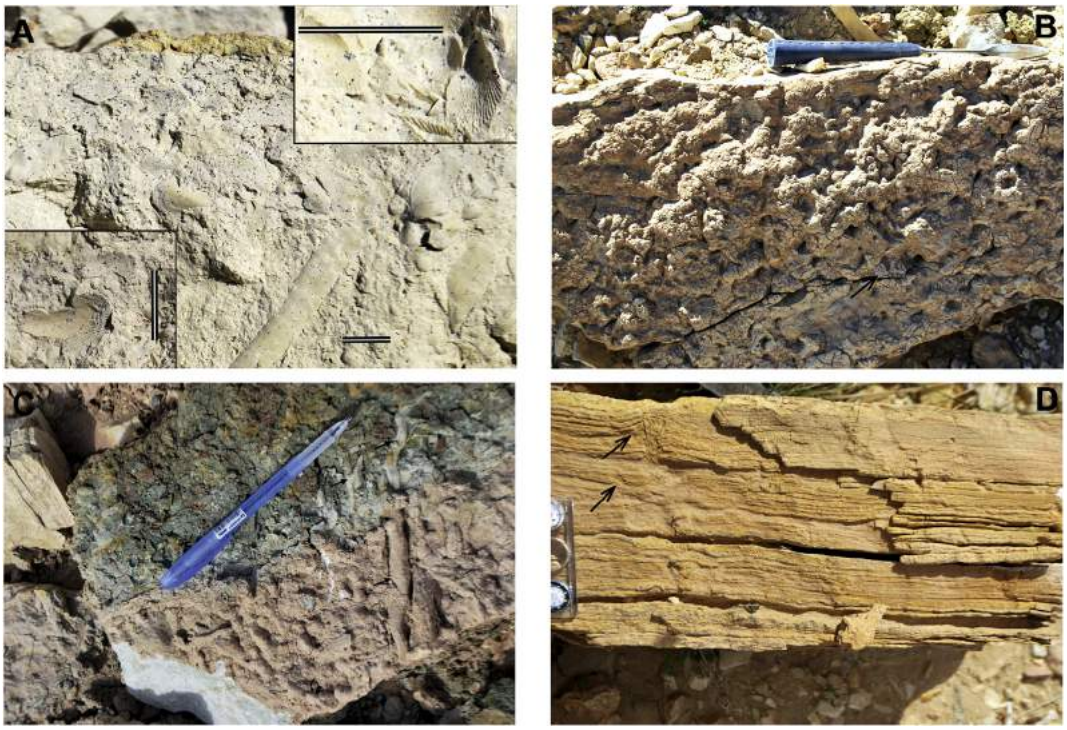

Fig. 9. Field photographs of some facies from the upper unit of El Rhelida Formation. A, Bioclastic limestone rich in *Pseudoptera anomala* (scale bar: 1 cm); B, Common deformed horizontal *Thalassinoides* trace fossils at the base of a bioclastic limestone bed; C, Horizontal branched burrows of *Ophiomorpha* at the basal surface of a limestone bed; D, Algal lamination deformed by dewatering structures (arrow).

The lower boundary is equivalent to the upper boundary of the El Rhelida Formation as above. Its upper boundary with the overlying Rhoundjaïa Formation is very sharp and represented by an abrupt lithologic and palaeo-environmental change. Here, the Mdaouer Formation can be broadly subdivided into two informal units:

4.2.1. Evaporitic unit

This unit is the major component of the Mdaouer Formation. It is mostly composed of red or pale green gypsiferous and unfossiliferous marlstones (Fig. 10A) with several, millimetre- to metre-thick, intercalated massive and laminated gypsum beds (Fig. 10B), occasionally with laterally continuous gypsum-and-algal beds (Fig. 10C). Centimetre-thick fine-grained sandstones, fenestral dolostone, mudstone with cubic evaporitic casts about 3 cm in average size (Fig. 10D), and bioclastic (bivalves and gastropods) limestone beds occur throughout the middle and upper parts of the unit.

4.2.2. Marlstone–limestone unit

This unit is recognized in all sections, as the uppermost five metres thick interval of the Mdaouer Formation. It consists of two brownish to greyish, hard, partly dolomitized, limestone beds intercalated with yellowish marlstones. The lower limestone bed is rich in bivalves and contains rare gastropods moulds. The upper limestone bed is well-stratified, with microbial laminites and well-preserved desiccation polygons (Fig. 10E–F). The bio-laminae had induced some little disruption of stratification, although scattered early-diagenesis deformation structures are also occurring as intraformational convoluting and sliding structures. The marlstone interval in between limestone beds contains a few and low-diversity smooth-shelled ostracode assemblage which mostly consists of *Paracypris* cf. *dubertreti* Bassoullet and Damotte, and *Pterygocythere*? *neknaffiensis* Andreu and Ettachfini. Gypsum levels are lacking within this unit.

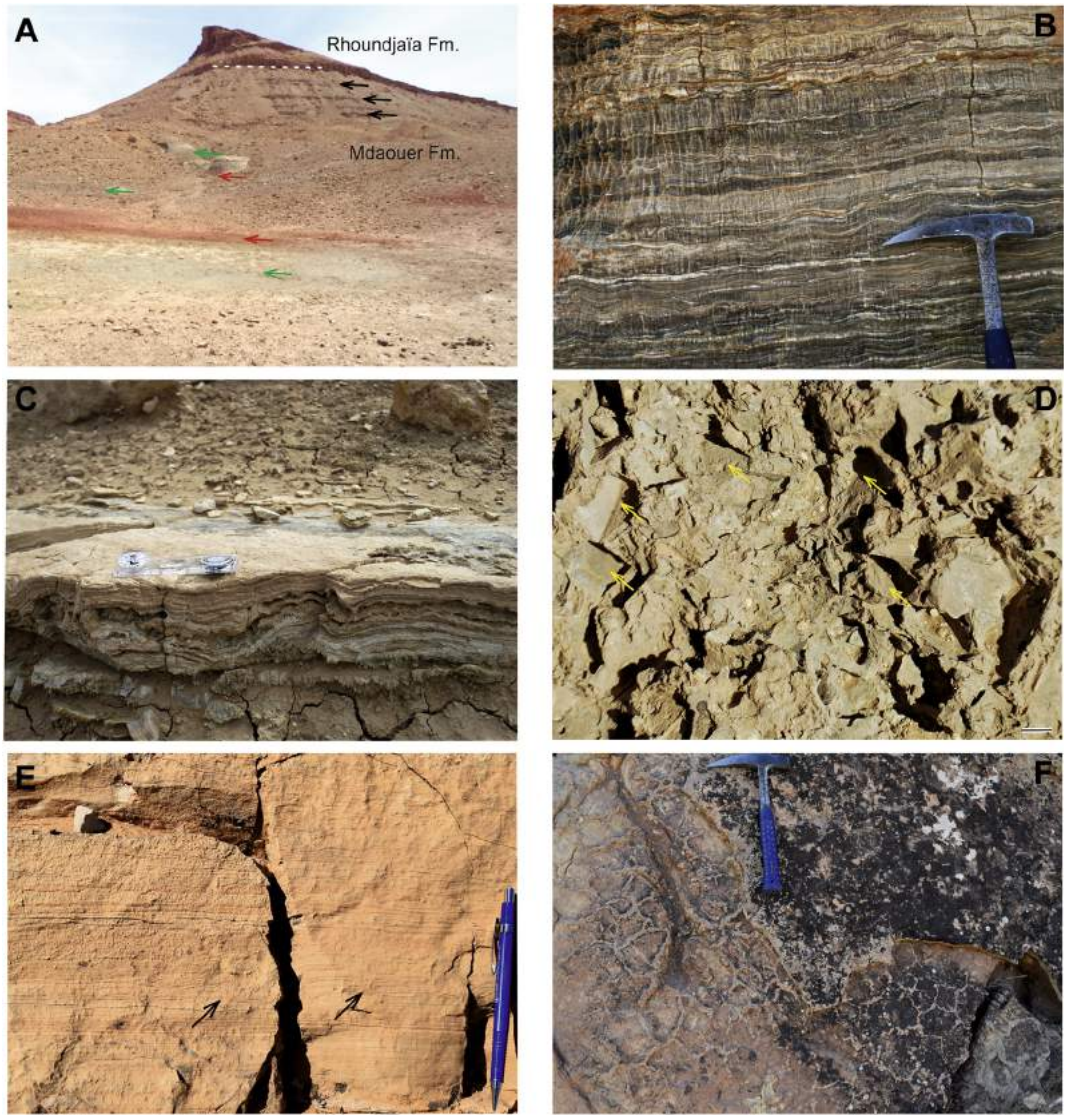

Fig. 10. Field views of the Mdaouer Formation. A, Alternation of red (red arrow) and green (green arrow) gypsiferous marlstones. Note the intercalation of tick massive gypsum beds (black arrow) near the top part of the formation; B, Laminated gypsum showing regular alternation of white gypsum laminae and dark lime-mud laminae; C, Irregular interlaminations of slightly undulating dark-coloured stromatolitic laminae and light-coloured gypsum laminae (ruler: 9 cm); D, Halite pseudomorphs in dolostone interbedded within the middle part of the Mdaouer Formation. (Djebel El Rhelida section), scale bar: 1 cm; E, Bio-laminated limestone bed at the uppermost part of the Mdaouer Formation. Note the soft-sediment deformation structures (arrow); F, Well-preserved desiccation cracks at the top surface of the previous limestone bed. (For interpretation of the references to colour in this figure legend, the reader is referred to the web version of this article.)

4.3. Rhoundjaïa Formation

The Rhoundjaïa Formation is a major carbonate entity within the Cretaceous successions of the Ksour Mountains. It was originally defined by Bassoullet (1973), from its type locality in Djebel Rhoundjaïa (from spoon-like = Rhoundjaïa in Berber language) near Ain Ouarka village (Fig. 1C).

Well-exposed in the three studied sections, its thickness ranges from 90 m in Djebel Mdaouer, to 100 m in Djebel Rhoundjaïa, and finally to 115 m in Djebel El Rhelida (Fig. 4). Overlying the Mdaouer Formation, the limit in between these two formations can be traced throughout the whole western Saharan Atlas due to a marked vertical lithofacies change from brownish algal limestones of the upper Mdaouer Formation to the conformably overlying, grey highly fossiliferous limestone of the Rhoundjaïa Formation. Such a boundary is obviously discernable within the landscape from its outcropping morphology. The overlying formation in the type locality is covered by Quaternary deposits. However, near Oued Djeraf (Fig. 1C), the upper boundary rests conformably and is defined by an abrupt change from the thin-bedded limestones of the uppermost Rhoundjaïa Formation to a red siliciclastic succession, consisting of clay-sandy-microconglomeratic alternations.

We recognised three informal units, mainly based on lithologic features, as follows:

4.3.1. Lower limestone unit

This unit corresponds to the 'lower limestone ledge' of former authors. Their base consists of thin brown highly bioturbated limestone bed with *Thalassinoides* burrow networks in Djebel El Rhelida. However, in Djebel Rhoundjaïa and Djebel Mdaouer, the lowest part of the unit consists of blue to dark grey shell concentration of small gryphaeid oysters [*Costagyra olisiponensis* (Sharpe) and *Rhynchostreon suborbiculatum* (Lamarck)], usually 5–25 cm thick, with sharp erosional base and laterally discontinuous (Fig. 11A). Based on its lithological composition and faunal content, the lower limestone unit can be subdivided, in all studied sections, into two distinctive parts:

The lower part consists mostly of grey massive limestone beds (0.8–5 m thick), showing a very homogeneous and pseudo-nodular appearance (Fig. 11B) with irregular stratification surfaces. It is

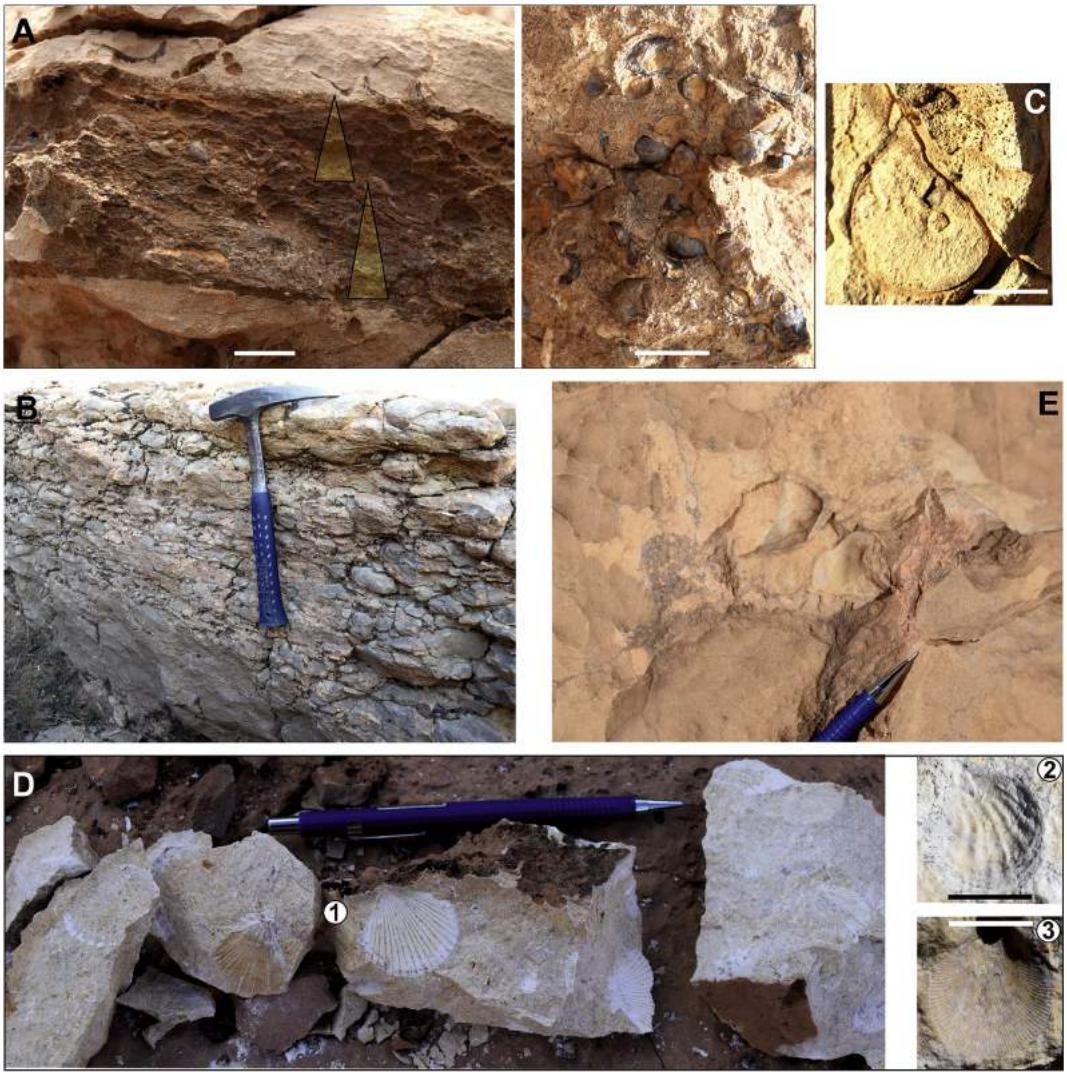

Fig. 11. Field photographs of the Rhoundjaïa Formation. A, Bioclastic bed very rich in small exogyrine oysters at the lowermost part of the lower limestone unit (scale bar: 2 cm). Note that the bioclast size decreases upwards; B, Homogeneous and pseudo-nodular beds at the basal part of the lower limestone unit; C, Ammonite *Neolobites vibrayeanus* found in situ (scale bar: 2 cm); D, Limestone bed rich in pectinid bivalve genus *Neithea* (1) in association with other bivalves species (e.g., 2 – external mould of *Plicatula ferry*, 3 – external mould of *Camptonectes curvatus*, scale bar: 2 cm); E, Mudstone–wackestone facies intercalated by thin bioclastic layer rich in *Rhynchostreon suborbiculatum* (Lamarck) at the upper part of the lower limestone unit.

commonly very fossiliferous. The fossil components are dominated by gryphaeid oysters [*Costagyra olisiponensis, Ceratostreon flabellatum* (Goldfuss), *Ilymatogyra africana* (Lamarck) and *Rhynchostreon suborbiculatum*] and other bivalves [*Plicatula auressensis* Coquand, *Plicatula ferryi* Coquand, *Neithea* sp., *Granocardium productum* (Sowerby), *Granocardium* (*Granocardium*) cf. *desvauxi* (Coquand), *Pholadomya* (*Pholadomya*) *pedernalis* (Roemer), and *Pholadomya* (*Pholadomya*) *vignesi* Lartet], gastropods [Cerithiinae indet., *Cimolithium tenouklense* (Coquand), *Ampullina* sp., *Strombus incertus* (d'Orbigny) of large size, and *Tylostoma* sp.] and echinoids [*Tetragramma variolare* (Brongniart), *Heterodiadema libycum* (Agassiz and Desor), and *Mecaster batnensis* Coquand]. Ammonites [*Neolobites vibrayeanus* (d'Obigny) (Fig. 11C), and *Calycoceras* (*Calycoceras*) *naviculare* Mantell] are subordinate. Microfacies documents a preponderance of skeletal components, a lack of non-skeletal grains, and displays low diversity: mudstones–wackestones (Fig. 13A–B) and rare packstones with ostracode valves, ophiuroids, benthic foraminifera (cf. *Dictyoconus* and *Frondicularia* sp.), planktonic foraminifera, pelagic crinoids (Roveacrinidae indet.), pithonellids, holothuroid sclerites and molluscan debris (gastropods, inoceramid shells, oysters and other unspecified bivalves). Among planktonic foraminifera *Asterohedbergella asterospinosa* (Hamaoui) is very common in the lower part of the succession.

In Djebel El Rhelida, the lower part of the lower limestone unit is capped by a well-stratified (40 cm thick) massive, yellowish-white bed rich in pectinid bivalve genus *Neithea* [*Neithea* (*Neithea*) *quinquecostata* Sowerby and *Neithea* (*Neithella*) *notabilis* (Muenster in Goldfuss)]. Secondary faunal elements are bivalves *Costagyra olisiponensis, Plicatula ferryi,* and *Camptonectes curvatus* (Geinitz). This *Neithea*-rich limestone (Fig. 11D) is followed by another brown bioclastic limestone horizon (10 cm thick), delivering poorly preserved ammonite specimens.

The upper part of the lower limestone unit is mainly composed of a brown to grey, hard limestone succession containing large internal moulds of gastropod *Strombus incertus* and oysters, such as *Ilymatogyra africana* and *Rhynchostreon suborbiculatum* (Fig. 11E). The succession shows a very homogeneous and massive appearance. Locally, bedding shows bioturbation, and *Thalassinoides* occurs at several levels. The base of the succession also displays trace fossils *Rhizocorallium* and *Planolites* (Fig. 12A–B).

In Djebel Rhoundjaïa and Djebel Mdaouer sections, the lower limestone unit is capped by a nodular ferruginous limestone bed, 15 cm thick, and rich in *Calycoceras* (*Calycoceras*) *naviculare*. In Djebel El Rhelida, its upper boundary is located at a highly bioturbated surface, below the vascoceratid-rich beds (Fig. 12C) and marl alternation of the second unit.

4.3.2. Middle marly unit

The middle marly unit ranges in thickness from less than 10 m in Djebel El Rhelida to more than 25 m in Djebel Rhoundjaïa and

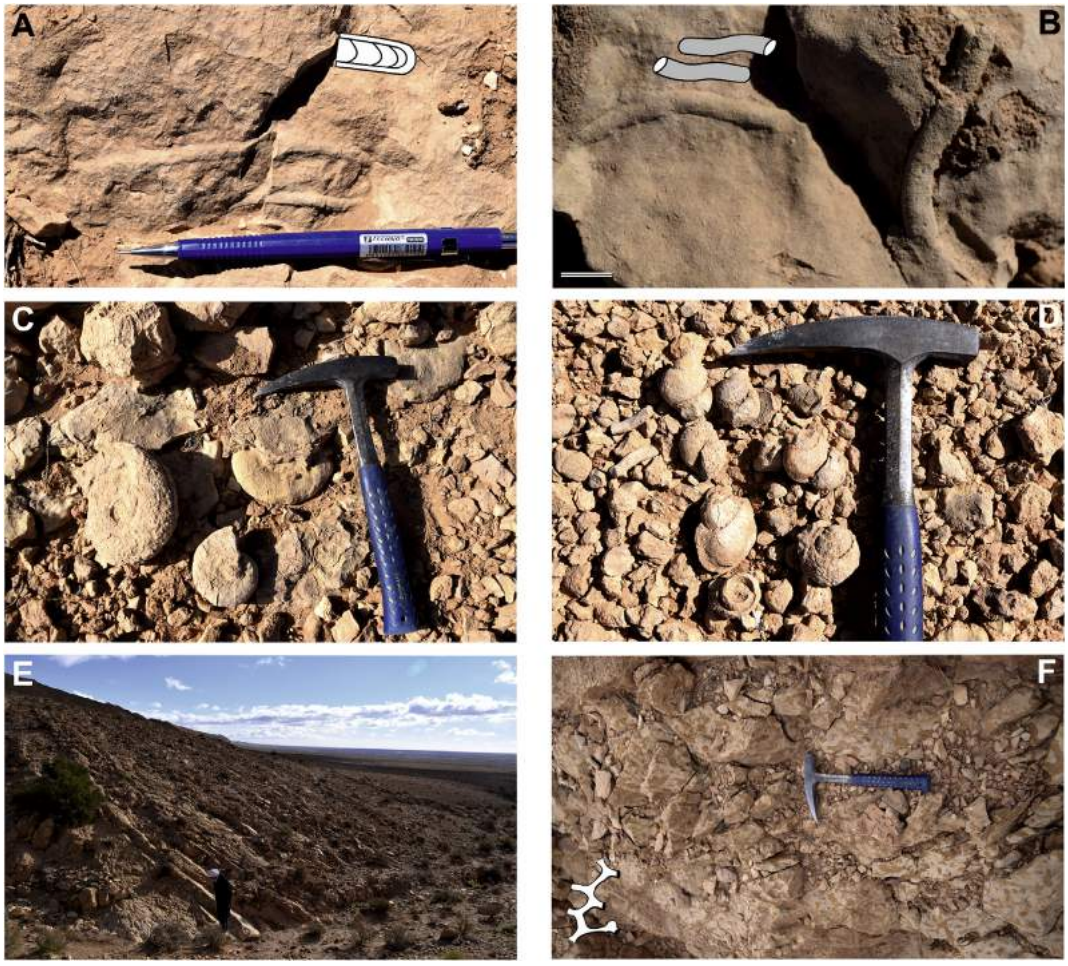

Fig. 12. Field photographs of the Rhoundjaïa Formation. A–B, Massive limestone showing *Rhizocorallium* (A) and *Planolites* (B) burrows at the upper part of the lower limestone unit (for B, scale bar: 1.5 cm); C–D, Vascoceratids (C) and tylostomids (D)-rich limestone at the lowermost part of the middle marly unit (Djebel El Rhelida section); E, Succession of thin and laterally continuous mudstone beds at the uppermost part of the upper limestone unit; F, Intensively bioturbated limestone with *Thalassinoides* burrows at the lowermost part of the upper limestone unit (Djebel Rhoundjaïa section).

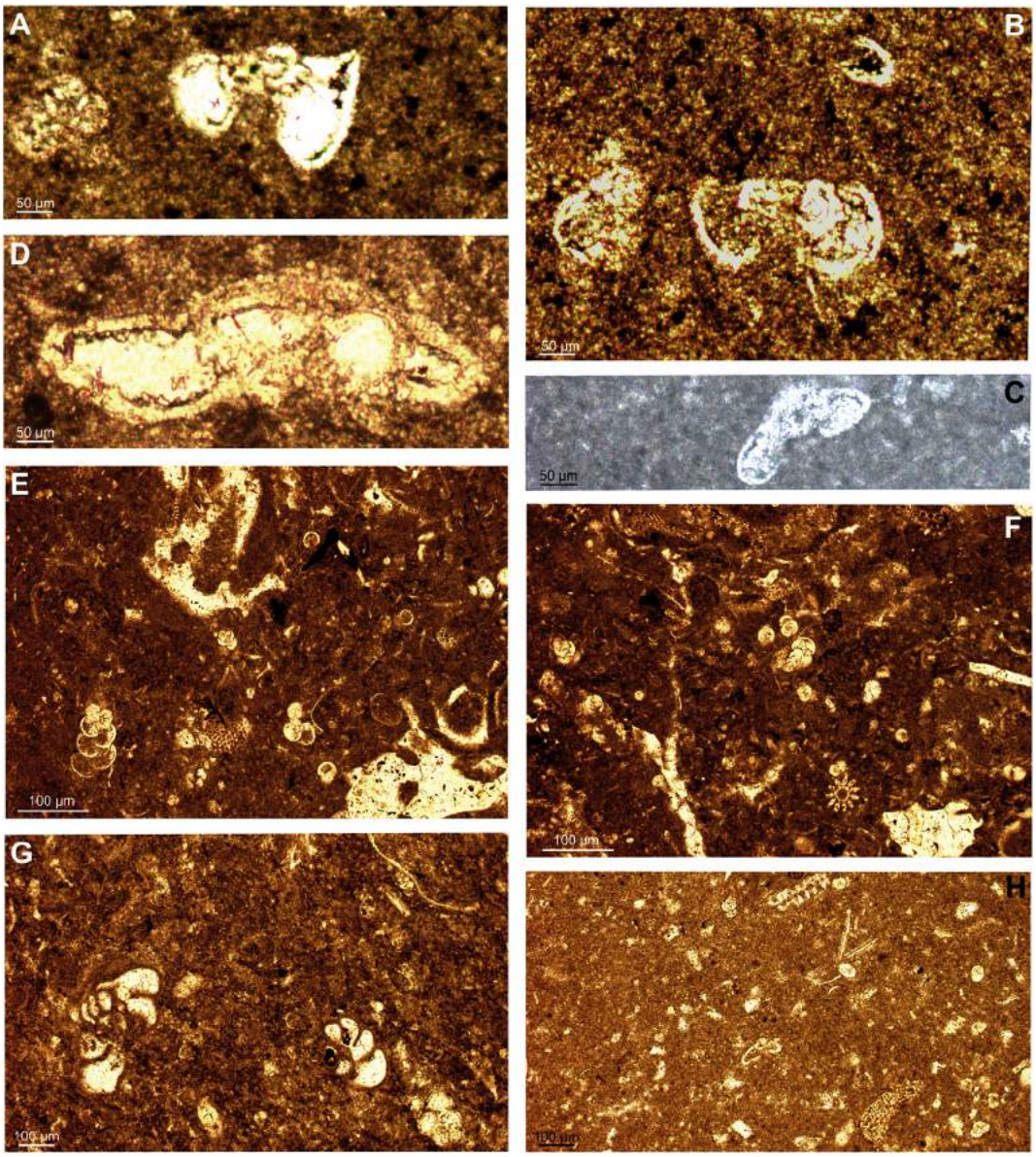

Fig. 13. Microfacies of the Rhoundjaïa Formation; A, Bioclastic mudstone–wackestone with section of *Asterohedbergella* sp.; lower limestone unit; B, Planktonic foraminiferal mudstone with *Whiteinella* sp.; lower limestone unit; C, Planktonic foraminiferal mudstone with *Whiteinella* sp.; middle marly unit; D, Bioclastic mudstone–wackestone with *Dicarinella* sp.; middle marly unit; E, Bioclastic mudstone–wackestone with heterohelicids, ostracode valves, ophiuroid and bivalves fragments; middle marly unit; F, Bioclastic wackestone with heterohelicids, ostracode valves and echinoid spines; middle marly unit; G, Mudstone with benthonic foraminifers (*Valvulammina picardi*) and bivalve sections; middle marly unit; H, Bioclastic mudstone–wackestone with planktonic foraminifers, pithonellids, echinoid spines and ophiuroid sections; middle marly unit.

Djebel Mdaouer. It consists of an alternation of white to yellowish soft, fossiliferous marlstone, and 5–7 beds of grey bioclastic limestone. These carbonate beds are hard, 0.20–2 m thick, and contain complete ammonites [*Nigericeras gadeni* (Chudeau), *Vascoceras durandi* (Thomas and Peron), *Vascoceras gamai* Choffat, *Fikaites subtuberculatus* (Collignon), and *Fikaites* cf. *varicostatus* Zaborski], several moulds of gastropods, in particular *Tylostoma cossoni* Thomas and Péron (Fig. 12D), and scarce bivalves and echinoderms such as *Anorthopygus michelini* Cotteau and *Orthopsis ovata* Coquand. Their microfacies shows a mudstone–wackestone texture with planktonic foraminifers [*Muricohedbergella delrioensis* (Carsey), *Heterohelix moremani* (Cushman), *Heterohelix reussi* (Cushman), *Asterohedbergella* sp., *Dicarinella* cf. *canaliculata* (Reuss), *Whiteinella archaeocretacea* Pessagno, and *Whiteinella praehelvetica* (Trujillo)], benthonic foraminifers [*Gavelinella berthelini* (Keller), *Valvulammina picardi* Henson, and *Frondicularia* sp.], ostracode valves [*Cytherella* gr. *ovata* (Roemer), and *Paracypris* sp.], ophiuroid ossicles, pelagic crinoids, pithonellids, echinoderm plates, gastropods, and bivalve fragments (Fig. 13C–H).

The interbedded marls delivered abundant benthonic foraminifers (*Gavelinella berthelini, Valvulammina picardi, Frondicularia* sp., and *Thomasinella* sp.), planktonic foraminifers (*Heterohelix moremani* and *Heterohelix reussi*) and very well preserved ostracode valves [*Bairdia* sp., *Haughtonileberis mdaouerensis* (Bassoullet and Damotte), *Cytherella* gr. *ovata* (Roemer), *Paracypris mdaouerensis* (Bassoullet and Damotte), *Cythereis algeriana* (Bassoullet and Damotte), and *Reticulocosta* gr. *tarfayaensi* (Reyment)].

4.3.3. Upper limestone unit

The upper limestone unit is about 45 m thick and consists entirely of carbonates showing vertical variations in faunal content

and stratonomy. It is well developed in Djebel El Rhelida where it can be divided into three distinctive parts:

The basal part of this unit is about 18 m thick. It mainly consists of a grey, yellow to cream, very hard, limestone which contains densely packed ammonites of late Cenomanian (Vascoceratidae) and early Turonian [*Pseudotissotia nigeriensis* (Woods) and *Choffaticeras sinaiticum* Douvillé] age. Petrographic analysis of thin-sections reveals mudstone–wackestone textures with rare benthonic foraminifers (*Gavelinella berthelini*, *Valvulammina picardi,* and *Cuneolina* sp.) and planktonic foraminifers (heterohelicids and hedbergellids), ostracode valves, calcispheres, pelagic crinoids (*Roveacrinus* sp. cf. *alatus* Douglas), ophiuroids, and diverse echinoderm bioclasts (plates and spines), bivalves and gastropods. The boundary between Cenomanian and Turonian ammonite beds is marked by a highly bioturbated surface showing a dense network of *Thalassinoides* and *Planolites* burrows.

The middle part is about 22 m thick and predominantly composed of brownish yellow, very hard, limestone, devoid of any macrofossils with the exception of a few bivalve debris. In the Mdaouer section, we found some small rudistid patches belonging to genus *Sauvagesia*.

The uppermost part is about 5 m thick and mostly consists of dark grey to bluish, thin laminated limestone beds (Fig. 12E) displaying thin continuous chert bands.

In the Djebel Rhoundjaïa and Djebel Mdaouer sections, the basal part of the upper limestone unit is dominated by a massive strongly *Thalassinoides*-bioturbated limestone (Fig. 12F), overlain by massive limestone beds devoid of any macrofossil relic. The uppermost part of the unit is eroded.

5. Biostratigraphic data and geochronological assignments

The biostratigraphy of the Cretaceous succession of the Ksour Mountains had been studied by Bassoullet (1973). The limited extent of some outcrops and the lack of diagnostic fossils in most localities did not always allow Bassoullet to deliver precise biostratigraphic assignments. Bassoullet (1973) assumed, without any hard evidence, a latest Albian (Vraconnian) age for the El Rhelida Formation; the overlying Mdaouer Formation was assigned to the lower Cenomanian; The Rhoundjaïa Formation was attributed to the upper Cenomanian-lower Turonian (Figs. 2 and 4). Bassoullet's late Cenomanian age was based on the presence of ammonite *Neolobites vibrayeanus*; and the early Turonian age was proposed thanks to the occurrence of ammonite *Vascoceras cauvini* (from the middle marly unit). However, this ammonite species is widely known from upper Cenomanian strata of central and northern Africa, the Middle East, and Peru (Nagm and Wilmsen, 2012). Actually, previous studies of the Ksour Mountains only recognized upper Cenomanian faunas.

Our recent fieldwork in the Ksour Mountains has been enabling us to precise the Upper Cretaceous biostratigraphy and geochronological assignments.

The lowermost part of the El Rhelida Formation, exposed in the valley of Oued Boudjihane, yielded vertebrate remains (*Spinosaurus aegyptiacus, Spinosaurus* sp., *Lepidotes* sp., *Mawsonia* sp., *Neoceratodus africanus,* and *Onchopristis numidus*) indicative of an early Cenomanian age, compared to the respective faunas of the "Grès rouges" Formation in the Guir Basin (Benyoucef et al., 2014, 2015), of the "Kem Kem" beds in eastern Morocco (Sereno et al., 1996; Cavin et al., 2010), and of the Bahariya Formation in Egypt (Stromer, 1914; Le Loeuff et al., 2012).

No biostratigraphically significant micro- or macro-fossils occur in the deposits of most part of the Mdaouer Formation. An early-middle Cenomanian age was assigned given their stratigraphic position in the section. These deposits are overlying the vertebrate levels of early Cenomanian age (lower El Rhelida Formation) and directly overlain by the deposits of the Rhoundjaïa Formation yielding *Neolobites vibrayeanus* (lower upper Cenomanian) at their lowermost part (Figs. 3–4). From a lithological point of view, the Mdaouer Formation is coeval to the lower-middle Cenomanian "Marnes à gypse inférieures" Formation of the Guir Basin (Benyoucef and Meister, 2015; Benyoucef et al., 2016). Furthermore, the marly interval within the uppermost part of the Mdaouer Formation yielded *Paracypris* cf. *dubertreti* Bassoullet and Damotte, and *Pterygocythere*? *neknaffiensis* Andreu and Ettachfini. In the South Tethyan margin, from Morocco to the Middle East, this ostracode assemblage indicates a middle to late Cenomanian age (Mebarki et al., 2016).

The lower part of the Rhoundjaïa Formation outcropping in every study section yields ammonites *Neolobites vibrayeanus* and *Calycoceras* (*Calycoceras*) *naviculare* both indicating the *Calycoceras guerangeri* Zone, of early late Cenomanian age (Meister et al., 2017).

From the occurrence of ammonites *Nigericeras gadeni, Vascoceras gamai, Fikaites subtuberculatus* (Mebarki et al., 2015), *Vascoceras durandi,* and *Fikaites* cf. *varicostatus*, the middle marly unit is ascribed to the uppermost Cenomanian. These species indicate the upper part of the *Metoicoceras geslinianum* and the *Neocardioceras juddii* ammonite zones.

In the basal levels of the upper limestone unit, a lower Turonian age was obtained due to newly found ammonites *Pseudotissotia nigerensis* and *Choffaticeras sinaiticum*. This ammonite assemblage corresponds to the upper part of the *Watinoceras coloradoense* Zone. Macro- and micro-fossils are generally scarce in the uppermost part of the Rhoundjaïa Formation, but a middle-late Turonian age cannot be discarded.

Precisely locating the Cenomanian-Turonian (C/T) stage boundary in the successions of the Ksour Mountains is rather difficult. Actually, no biostratigraphic markers occur within this transition. The C/T boundary is formally defined by Kennedy et al. (2005) at the FO of ammonite *Watinoceras devonense* at the base of Bed 86 in the Global Stratotype Section and Point (GSSP) of Rock Canyon Anticline (Pueblo, Colorado, USA). Unfortunately, *W. devonense* has not been found so far in South Algeria, as is the case for most C/T sections in other countries that are more expanded than that at Pueblo; e.g., the Ganuza section in Spain (Lamolda et al., 1997) and the Westphalia sections in Germany (Lehmann, 1999).

So, a stratigraphic gap might be considered in the Ksour Mountains at least for the lower Turonian (*Watinoceras devonense* and *Pseudaspidoceras flexuosum* zones), because late early Turonian ammonites (uppermost *Watinoceras coloradoense* Zone) *Pseudotissotia nigeriensis* and *Choffaticeras sinaiticum* are found in deposits directly overlying the uppermost Cenomanian strata (*Neocardioceras juddii* Zone). This possible gap could be most likely related to a submarine non-deposition. As observed in the field, a marked bioturbated surface documents a possible hiatus between the top of the grey limestones including upper Cenomanian ammonites and the overlying yellow limestones that represent the base of the lower Turonian. Such a hiatus of this magnitude was also reported in the Tinrhert Basin (Zaoui et al., 2016), in the Middle East (Buchbinder et al., 2000), in Sinai in Egypt (Bauer et al., 2003), and in the Sergipe Basin in Brazil (Walter et al., 2005).

6. Facies analysis

6.1. Description and interpretation of facies

Based on field observations, such as lithology, sedimentary structures, textures, bed thickness, bedding geometry, and fossils and/or trace fossil content, supplemented by microfacies analysis, twenty-eight distinctive sedimentary facies types (FT1 to FT28) were identified, the sedimentological description and interpretation of which are summarized in Table 1. Some characteristic outcrop and microfacies photographs are presented in Figs. 5–13.

Table 1
Description and sedimentological attributes of litho-facies identified in Cenomanian-Turonian deposits of the Ksour Mountains.

Facies type (FT)	Description and range	Interpretation and environmental significance
FT1. Microconglomerate	**Lower part of the El Rhelida Fm.** Thin massive tabular to lenticular beds (10–30 cm thick). Sub-rounded to rounded pebble, resistant quartz grains, vertebrate debris and other lithic materials within fine-grained sandstone (Fig. 6E–F). Lower contacts are sharp and erosive, overlying oxidized sandstone (FT2); upper contacts are sharp with overlying bioturbated sandstone (FT3).	Transgressive lag deposit, as suggested by its position above the continental oxidized sandstone (FT2) and below the marine (transgressive) strongly bioturbated sandstone (FT3). It corresponds to the "simple transgressive lags" of Cattaneo and Steel (2003).
FT2. Oxidized sandstone	**Lower part of the El Rhelida Fm.** Thin fine-grained sandstone beds (5–15 cm thick) extending laterally for several hundred metres. Outcropping, they are characterized by their reddish hue due to haematite cementation. Fauna, bioturbation and sedimentary structures have not been observed (Fig. 5A).	Haematite cementation suggests a relatively prolonged subaerial exposure. Thus, the oxidized sandstone can be related to subaerial exposure.
FT3. Massive bioturbated sandstone	**Lower part of the El Rhelida Fm.** Fine-grained, brown to red sandstones beds (10–30 cm thick) displaying moderate to intense bioturbation. The ichnofossil association contains *Bergaueria, Helminthopsis, Lockeia, Planolites* cf. *beverleyensis, Planolites montanus, Phycodes, Rhabdoglyphus*, and *Spirophycus*. Some beds are intensively bioturbated by large *Thalassinoides* (Fig. 7A) and bioturbation often obliterates primary sedimentary structures.	Diversity and intense bioturbation reflect regular marine conditions and a low rate of sedimentation. The trace-fossil association at hand characterizes some littoral rock-ground environments (mixed Skolithos-Cruziana ichnozone, Seilacher, 1967). They correspond to suspension fallout during fair-weather conditions occurring between the high-energy current depositions (or storm deposits, FT1).
FT4. Structureless sandstone	**Lower part of the El Rhelida Fm.** Fine- to medium-sized sand quartz grains, moderately sorted sandstone. The beds (0.50–1 m thick) are tabular, devoid of any morphological features, biogenic structures, or fossils. The top part of beds is partly rippled with symmetrical wave ripples.	The massive nature is inferred from the loss of primary stratification through bioturbation processes or rapid sedimentation disallowing formation of primary internal layering. The scarcity of biogenic structures and fossils supports a deposition under high-energy conditions. This facies originates in the lower shoreface environments. Presence of some symmetrical wave ripples indicates that high-energy conditions were separated by intervals of slow deposition.
FT5. Cross-bedded sandstone	**Lower part of the El Rhelida Fm.** Yellowish white to brownish yellow, unfossiliferous, fine to medium sandstone beds (10–80 cm thick), with non-erosional base, without any recognizable trend in granulometry. Grains are moderately sorted, sub-angular to sub-rounded. Presence of horizontal lamination, trough cross-stratification, with low-angle as well as steep planar cross bedding, locally with herring-bone structures. Reactivation surfaces are common and bioturbation is rare to absent (Fig. 5B–E).	The high maturity of sands, sub-angular to sub-rounded quartz grains, cross-stratification, faunal scarcity, all point to deposition under moderate to high-energy conditions (Pettijohn et al., 1987). The presence of reactivation surfaces indicates fluctuating flow velocities (Nio and Yang, 1991). Low-angle planar cross-bedding may be correlated with the zone of wave swash, whereas steep planar cross-bedding is interpreted as caused by longshore currents. They indicate a high-energy nearshore environment. Low-diversity and density of fossil traces suggest environmental stress, probably related to high sedimentation rates and brackish conditions. This facies was most probably deposited in the upper shoreface.
FT6. Hummocky cross-stratification sandstone	**Lower part of the El Rhelida Fm.** Fine- to medium-grained, well-sorted and hummocky cross stratified sandstone beds (40–60 cm thick). The hummocks consist of cross-stratified sets with low angle dips. They have erosional bound tops and bases, and are internally laminated with laminae parallel to the lower surface (Fig. 5F–G and Fig. 6A).	According to Walker (1990), hummocky cross stratifications are generally associated with storm-enhanced wave action below fair-weather wave base.
FT7. Rippled sandstone	**Lower part of the El Rhelida Fm.** Reddish, quartz fine sandstone beds (5–50 cm thick) that can be traced laterally over tens of metres. The characteristic sedimentary feature is ripple lamination and lamination formed by aggradation of both symmetrical and combined flow (slightly asymmetrical) wave ripples (Fig. 5G and Fig. 6B).	Symmetrical ripples are the result of symmetrical oscillatory waves, whereas the asymmetrical ripples are formed by shallower translatory waves. This facies bears genuine evidence of wave action (Harms et al., 1982; Craft and Bridge, 1987), typical of the lower shoreface environment (Spalletti and Del Valle, 1990) or the friction-dominated zone (Swift and Niedoroda, 1985).
FT8. Thin sandstone	**Mdaouer Fm.** Greenish quartz sandstones occur as cm-thick layers on erosional surfaces in green and reddish claystones. The base of each bed is irregular and scoured, the top frequently covered with oscillation ripples. Phosphatic grains as well as reworked claystone pebbles are also occurring. Occasionally, undiagnostic trace fossils are found on the upper sandstone bedding planes.	The thin sandstone layers appear to record rapid and wide spreading inundation of an extensive mudflat.
FT9. Green and reddish claystones	**Upper part of the El Rhelida Fm. and major part of the Mdaouer Fm.** Green-grey and red unfossiliferous claystones (a few cm-up to metre-thick), occasionally preserved lamination, including horizons with mud cracks, a few, cm-thick sandstone, dolostone with well-developed evaporate-crystal casts and bioclastic limestone beds.	Greenish claystones generally suggest a reducing environment, caused by more frequent flooding or by ephemeral lacustrine conditions. In contrast, red claystones probably represent longer exposed mudflats with less frequent flood events. The thin multi-coloured claystones intercalated into marine bioclastic facies could result from mechanical transport of clays during times of heavy rain, as described by Warren (1982). Thicker claystones may represent very distal end members of river floods, similar to flood deposits brought into the modern West Australian MacLeod salina by ephemeral streams (Logan, 1987). This facies is also similar to inland sabkhas and mudflat deposits

(*continued on next page*)

Table 1 (*continued*)

Facies type (FT)	Description and range	Interpretation and environmental significance
		described by several authors (e.g. Eugster and Hardie, 1975; Handford, 1982; Kendall, 1984).
FT10. Unfossiliferous and gypsiferous marlstones	**Major part of the Mdaouer Fm.** Greenish or red in colour, unfossiliferous and gypsiferous marlstones (a few cm-up to metre-thick, Fig. 10A), between the gypsum and limestone horizons.	Calm-water conditions allowing the settling down of fine particles in suspension were the site of deposition of such facies. The occurrence of gypsum in the marlstones may indicate arid conditions in supratidal sabkha settings.
FT11. Low-diversity marlstones	**Uppermost part of the Mdaouer Fm.** Yellowish poorly fossiliferous marlstones with rather monospecific, smooth-shelled ostracodes; intercalated in between two limestone beds	This facies deposited from suspension in quiet waters, under low-oxygen shallow marine conditions, especially under restricted conditions due to the presence of low-diversity shallow-water biota, while occasional fresh-water input can be assumed. The stratigraphic relationships with adjacent facies support such an interpretation.
FT12. Highly fossiliferous marlstones	**Rhoundjaïa Fm.** Monotonous white to yellowish marlstones, in packages up to 2 m thick, highly fossiliferous with ostracodes, benthic and planktonic foraminifers. They alternate with limestones beds rich in benthic and pelagic fauna.	Low-energy open-marine conditions, based on its skeletal grain and its interbedding with deep-marine fossiliferous limestones.
FT13. Algal laminated limestones and dolostones	**El Rhelida Fm. and Mdaouer Fm.** Well-preserved gently undulating to planar laminated, locally massive, greyish or brown limestones characterized by fenestral and microbialite laminae occurring as thin beds (10–40 cm thick), mostly extend laterally over a long distance. Micro-tepees and dewatering structures, mud cracks and ripples in some beds are commonly observed (Fig. 8A, 9D, Fig. 10E–F). Fossil content and bioturbation are lacking.	Fenestrae ('birdseye') structures originate from the shrinkage of microbial laminae during desiccation, and from gas generated by microbial decay (Shinn, 1983). The laminated rocks are interpreted as cyanobacterial laminites or stromatolites. Micro-tepee structures and isolated mud cracks interrupt the deposition and suggest repeated periods of emergence and subaerial exposure. So, this facies suggests an upper intertidal to lower supratidal depositional environment.
FT14. Fenestral mudstone/dolostone	**El Rhelida Fm. and Mdaouer Fm.** Light-brown to grey mudstone beds (5–20 cm thick), laterally persistent. The facies appears massive but, on weathered surfaces, shows faint traces of parallel lamination. The most important structures and sediment fabrics include fenestral fabrics (birdseyes). The top surfaces show mud cracks, rhombic ripple marks and rain-drop imprints (Fig. 8C–D).	This facies corresponds to facies SMF-23 of Wilson (1975) and Flügel (2010). It suggests partial or complete subaerial exposure as evidenced by wetting and drying of sediments in a low energy, restricted intertidal to lower supratidal environment (James, 1979; Wilson and Evans, 2002). Similar sediments are forming nowadays on supratidal flats of Florida and the Bahamas and on sabkha flats of the Persian Gulf (Shinn, 1986).
FT15. Limestone/ dolostone with evaporite casts	**Mdaouer Fm.** Greenish-grey sterile, homogeneous dolomitic mudstones beds (a few cm to 40 cm thick), with evidence of subaerial exposure such as vugs and desiccation cracks, containing cube-shaped moulds, commonly less than 2 cm but occasionally up to 3 cm in size, filled (or not) by mudstone and carbonate pseudomorphs after cubic minerals (probably halite, Fig. 10D). The surface often presents hard ferruginous crusts.	The abundant relics of primary to early diagenetic evaporites (halite crystals) imply temporary hypersaline conditions related to episodic flooding of the depositional area by marine waters (Aigner and Bachmann, 1989; Paik and Kim, 1998; Hofmann et al., 2000). This lithofacies is interpreted as a supratidal deposit. Ferruginous crusts merely reflect a sedimentary break.
FT16.Gypsum-algal lamination	**Mdaouer Fm.** Gypsum-algal beds (10–60 cm thick) interbedded within gypsum marlstone and consist of millimetric regular alternations of light-coloured gypsum and brownish lime-mud laminae (microbial mats, Fig. 10C), thickness of each lamina ranges from <1 mm to a few millimetres. The intercalated algal laminae are uneven in thickness, wavy, disrupted, and form discontinuous bands.	The laminated mats formed in a shallow marginal marine salina along a supratidal flat. Interlamination with gypsum indicates that the growth of algal mats took place on the bottom during phases of dilution of saline water and low salinity rates, when gypsum precipitation ceased (Schreiber et al., 1982; Aref et al., 1997).
FT17. Laminated gypsum	**Mdaouer Fm.** Pale white to grey gypsum beds (50–160 cm thick). Very thin evaporitic laminae are alternating with thinner dark lime-mud laminae (organic material, possibly algal mats) (Fig. 10B). The laminated structure of this facies shows local deformation and overturning. Rhythmic couplets are distinct, but irregularly spaced.	This facies seems to represent a suite of inter- to supratidal flats with intermittent episodes of flooding and subaerial exposure.
FT18. Structureless gypsum	**Mdaouer Fm.** Light grey or white, but also greenish or reddish, structureless gypsum beds (a few cm to 1.70 m thick) showing sharp contact with the gypsiferous marlstones (FT10).	The occurrence of gypsum interbedded in the gypsiferous marlstones facies can be related to an arid climate in a supratidal setting (Shinn, 1983).
FT19. Thin bioclastic limestone intercalations within green claystones and marlstones	**Upper El Rhelida Fm. and sporadically Mdaouer Fm.** Light grey bioclastic lime mudstone beds (10–25 cm thick) rich in bivalves and gastropods; sharp erosive basal surfaces and sharp upper surface, intercalated between gypsiferous marlstones, bio-laminated limestone and gypsum facies. The basal part of beds is characterized by lenticular shell concentrations within a clast-supported fabric (packstone). Bioturbation is scarce, though micrite-filled millimetric burrows may occur (Fig. 9A).	Facies FT19, associated with the tidal flat deposits of FT10, FT13, and FT18, is characterized by a marine faunal content. It originated through an influx of marine water in another tidal environment. The driving force to bring that water could be extreme storm events.
FT20. Oyster shelly limestone	**Rhoundjaïa Fm. (lower limestone unit)** Blue to dark grey, hard bioclastic limestone bed (5–25 cm thick), with sharp erosional base and laterally discontinuous (Fig. 11A). The bioclastic content is restricted to small-sized disarticulated or strongly reworked nearly monospecific oyster shells embedded in a fine limestone matrix (wackestone–packstone). FT20 overlies shallow marine deposits of FT13 and is overlain by FT21 formed in relatively deep environments. It can be intercalated within the FT 23.	These characteristics indicate high energy deposits (Tucker and Wright, 1990; Flügel, 2004), and the combination of a sharp erosive base and reworked shells is characteristic of event deposits (Einsele et al., 1996). On a shallow platform, storms are the most likely phenomenon to cause such high-energy deposits (Aigner, 1982).
FT21. High-diversity fauna limestone	**Rhoundjaïa Fm. (lower part of the lower limestone unit)** Grey massive beds (0.8–5 m thick), showing a very homogeneous and	The diversity of the fauna shows that the primary environment had good water circulation (open marine),

Table 1 (*continued*)

Facies type (FT)	Description and range	Interpretation and environmental significance
	pseudonodular appearance with irregular stratification surfaces; very fossiliferous. The components are dominated by benthic fauna [bivalves (oysters, plicatulids, pectinids, cardiids and pholadomyids), gastropods (cerithiids, ampullinids, aporrhaid and tylostomids) and echinoids (diplopodiids, heterodiadematids and hemiasterids)] and pelagic fauna (ammonite *Neolobites*). In thin section, mudstone–wackestone texture includes pelagic crinoids, ophiuroids, calcispheres, benthic and planktonic foraminifera, ostracodes and bivalve sections, with sparse calcareous green algae.	warm and normal salinity and oxygen content within the water column and the sediment surface. The large amount of lime mud suggests that this facies type reflects slow and continuous sedimentation under low- to medium-energy.
FT22. *Neithea*-rich limestone	**Rhoundjaïa Fm. (middle part of the lower limestone unit)** Yellowish-white massive bioclastic limestone (40 cm thick) comprising a nearly monogeneric assemblage of the pectinid bivalve *Neithea* (Fig. 11D). The texture is micritic wackestone to packstone. *Neithea* shells are disarticulated, with a relatively low degree of abrasion and breakage. Minor faunal elements are plicatulids and oysters. The lower surface of bed is erosive and no sedimentary structures are visible.	In North Africa, the pectinid bivalve genus *Neithea* is found mainly in carbonate rocks representing shallow-marine environments. The erosional surface and the texture of the monogeneric bivalve concentration are indicative of sedimentation in wave-dominated shallow seas above the storm-wave-base and below the fair-weather wave-base.
FT23. Massive limestone	**Rhoundjaïa Fm. (upper part of the lower limestone unit)** Grey massive bioclastic limestone (0.5–3 m thick) of mudstone –wackestone texture. This facies yields only benthic fauna such as pectinids, gryphaeids, ostracodes and benthic foraminifers. Trace fossils are less common: some *Planolites* and *Rhizocorallium* are seldom found (Fig. 12A–B).	According to the presence of lime-mud supported texture, FT 23 was probably deposited in a low energy conditions (Flügel, 2010). Their palaeontological and ichnological content indicates a shallow marine environment.
FT24. Bioturbated limestone	**Rhoundjaïa Fm. (middle part of the lower limestone unit and lowermost part of the upper limestone unit)** Massive, grey micritic wackestone beds (a few cm to more than 1 m thick), displaying frequent anastomosing *Thalassinoides* leading to an almost complete sediment homogenization (Fig. 12F).	Abundance of *Thalassinoides* burrows in the micritic limestones indicates a soft substrate, low-water energy, fully oxygenated bottom-water, normal marine salinities, perhaps relatively lowered rates of sedimentation and considerable infaunal activity (Coffey and Read, 2004). It also suggests an intertidal to shallow subtidal regime (Bromley, 1967). According to Strasser et al. (1999), highly bioturbated carbonates indicate a shallow marine environment and suggest a low sedimentation rate.
FT25. Rudistid limestone	**Rhoundjaïa Fm. (upper limestone unit, Mdaouer section)** Dark-grey massive, tabular limestone bed (30–60 cm thick) including small isolated rudist patches dominated by genus *Sauvagesia*. Rudist shells are in life growth position or, in some cases, slightly oblique, both intact and fragmented. They are mostly embedded within lime-mudstone matrix with benthic foraminifers.	Faunal component and textural features suggest that this facies was deposited in normal marine upper subtidal environments with low to moderate water energy conditions; It can be assigned to small rudist patch reefs.
FT26. Cephalopod mudstone	**Rhoundjaïa Fm. (uppermost part of lower limestone unit, middle marly unit and lowermost part of the upper limestone unit in El Rhelida section)** Grey to brown nodular ammonite-rich limestone beds (10–70 cm thick) extending laterally over several hundred metres. The microfacies is lime mud-dominated rich in well-preserved ammonites, calcispheres, skeletal fragments, sponge spicules and pelagic foraminifers. Subordinate taxa are smaller benthic foraminifers.	The cephalopod facies has a mud-supported rock fabric, indicating deposition under rather low-energy conditions, below regular wave base (Wilson, 1975; Geel, 2000). Deeper-water and fully marine conditions are indicated by large amounts of well-preserved pelagic fauna.
FT27. Mudstone devoid of macrofossil.	**Rhoundjaïa Fm. (middle part of the upper limestone unit)** Dark grey fine-grained limestone beds (0.80–2 m thick) nearly devoid of any macrofauna. In thin sections, within a mudstone–wackestone texture, are occurring calcispheres, sponge spicules, and pelagic crinoids, fragments of echinoids, ostracodes, benthic foraminifera and planktonic foraminifera such as hedbergellids, whiteinellids and heterohelicids (Fig. 13).	The textural types of limestones indicate that this facies was probably deposited in a low energy environment (Flügel, 2010). Components such as pelagic crinoids, planktonic foraminifers and sponge spicules, indicate open marine setting, at least below storm wave base (Payros et al., 2010; Gorican et al., 2012).
FT28. Thin limestone –mudstone	**Rhoundjaïa Fm. (topmost part of the upper limestone unit)** Dark-grey massive, tabular limestone bed (10–30 cm thick) extending laterally over several hundreds of metres. The limestones show various degrees of silicification. In the less silicified parts, the cherts display a nodular, cauliflower-shaped pattern; in the more silicified parts, thin discontinuous chert bands (less than 20 cm thick) are commonly developed parallel to bedding (Fig. 12E). Microscopic investigation reveals that this lime-mudstone facies is dense micrite with scattered skeletal grains (bivalves), showing parallel lamination in places.	The fine-grained matrix suggests a low-energy hydrodynamic regime below fair-weather wave base in a distal subtidal environment.

6.2. Facies association and depositional settings

The distribution of these twenty-eight sedimentary facies within the succession led to coin seven facies associations (FA1 to FA7) which were, in turn, attributed to their respective position environment in three distinct sedimentary systems: mixed silicoclastic-carbonate system, mixed carbonate-evaporite system, and carbonate system.

6.2.1. Mixed silicoclastic-carbonate system

This sedimentary system is well-documented in the El Rhelida Formation, with two distinct facies associations: FA1 and FA2:

Facies association FA1: clastic foreshore–shoreface

This facies association is only found in the lower part of the El Rhelida Formation. It consists mostly of fine- to medium-grained sandstone (FT3 to FT7) with reddish to greenish claystone (FT9) and limestone/dolostones (FT13 and FT14), and minor microconglomeratic (FT1) and oxidized sandstone (FT2). On the whole, this facies association originated in a marginal to shallow-marine setting and suggests deposition under different flow regime conditions. It provides evidence of tidal currents and deposition by oscillatory flow

conditions in tide-and-wave dominated shoreline environments (Fig. 14A).

Herringbone cross beddings (FT5) indicate reversals in current direction typical of tidal regimes (Klein, 1970). Reactivation surfaces (FT5) are also described from tidal environments as a result of lee-face modification of bedforms by subordinate tidal currents (Ladipo, 1986). Hummocky cross-stratification (FT6) and wave ripple cross lamination (FT7) are both reflecting conditions of intense oscillatory flows that can be related to lower shoreface environments. Fair-weather periods are characterized by widespread bioturbation (FT3) seawards the upper shoreface. During the most severe storms the lower shoreface itself was the siege of winnowing phases, resulting in pebble lags material (FT1). The oxidized sandstone (FT2) and shallow marine carbonate levels (FT13 and FT14), in between the siliciclastic facies, were deposited in foreshore to backshore settings. They indicate phases of decreasing accommodation space and of suspension of continental supply of detrital material.

This lithofacies assemblage also partly resembles the "Grès rouges" Formation in the Guir Basin with similar vertebrate remains assemblages described by Benyoucef et al. (2015). This further supports the idea of potential regional correlation: part of the lower El Rhelida unit was deposited under marginal marine to brackish water conditions likewise the uppermost part of the "Continental intercalaire" (Benyoucef et al., 2014).

Facies association FA2: low-lying coastal mudflat

The upper part of the El Rhelida Formation is represented by multi-coloured (reddish and green) mostly massive claystones (FT9) defined herein as mudstones. Reddish mudstone intervals are dissected occasionally by small channels or interbedded to unconfined sheet-sandstones (FT8). Green mudstone intervals are sometimes interspersed by rare intercalations of few decimetres thin tabular carbonate beds, characterized by abundant marine fauna (bivalves and gastropods, FT19) or presenting evaporitic crystals (FT15). No gypsum bed was found.

The multi-coloured mudstones are interpreted as deposited in a low-lying coastal mudflat. The scarcity of primary sedimentary structures is easily explained by post-depositional bioturbation by

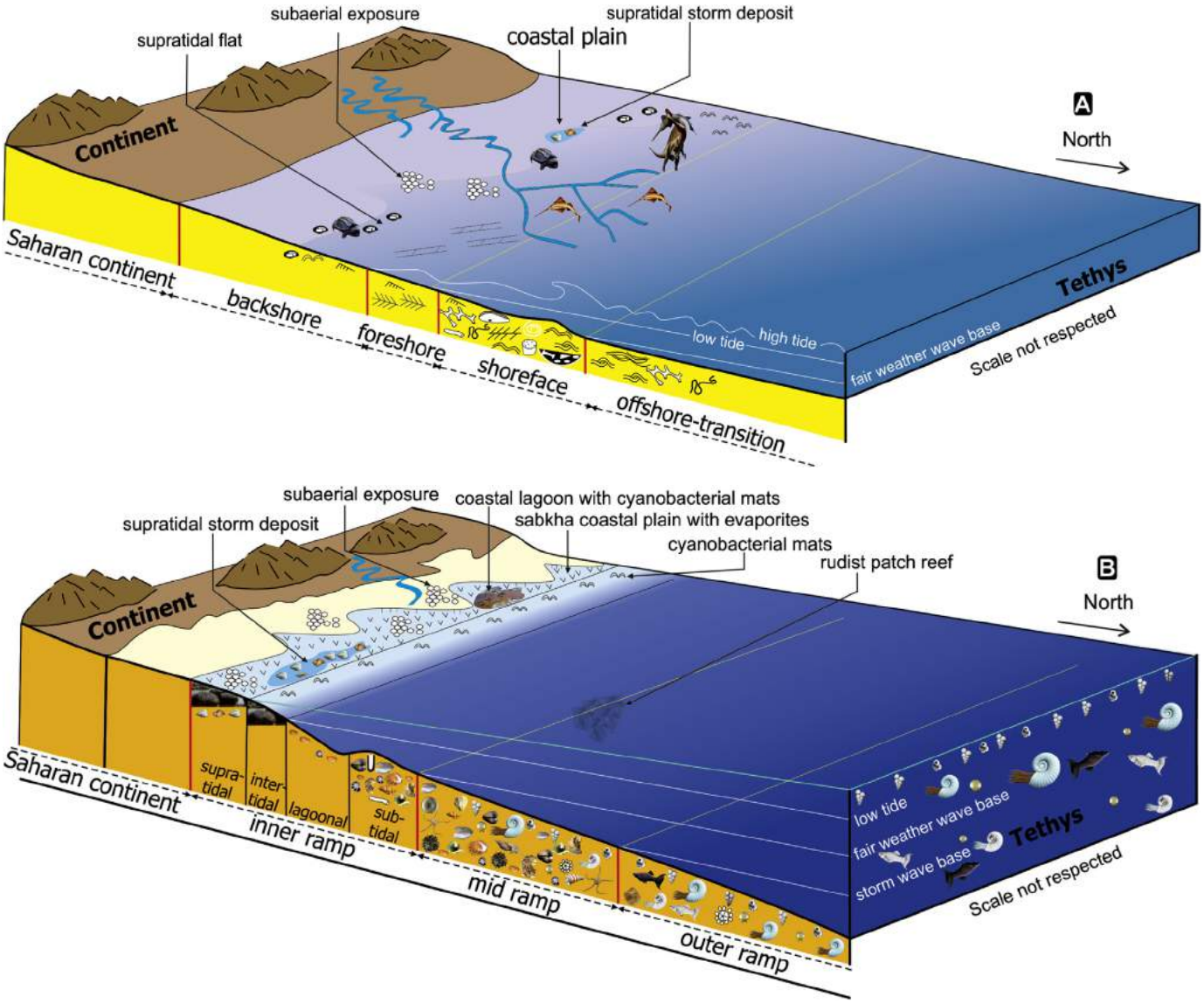

Fig. 14. Schematic depositional model diagram of the Cenomanian–Turonian sediments in the Ksour Mountains. A, Palaeo-environmental model of the mixed siliciclastic-carbonate unit (El Rhelida Formation); B, Palaeo-environmental model of the claystone–limestone unit (El Rhelida Formation), Mdaouer Formation and Rhoundjaïa Formation. The fair-weather and storm wave bases are placed after Burchette and Wright (1992).

plants and/or animals, as well as seasonal wet and dry alternations over long periods of non-deposition and/or erosion in the low-lying mudflat (Reinhardt and Ricken, 1999; Ghosh et al., 2006). Occasionally preserved lamination suggests that subaqueous deposition occurred, at least in some cases, in standing pools of water of an ephemeral nature, under very low-energy conditions (Aigner and Bachmann, 1989). The rare carbonate layers with evaporitic clasts can be associated with similar sub-environments. Reddish mudstones probably represent the very distal end members of river floods (element of Miall, 1985) and were deposited as suspended load from waning flows in the lowest lying area of a distal dryland river system (Tunbridge, 1984; Aigner and Bachmann, 1989). The intercalated thin tabular carbonate beds with marine skeletal, interrupting the regular fine clastic sedimentation, indicate small marine ingressions by storm surges resulting in extensive sea-water flooding.

6.2.2. Mixed carbonate-evaporite system

This sedimentary system constitutes significant parts of the Mdaouer Formation, with the following facies association:

Facies association FA3: coastal sabkha evaporites

This facies association is composed essentially of gypsum layers (FT17 and F18) alternating with unfossiliferous and gypsiferous marlstones (FT10). Subordinate laminated mudstones (FT13), fenestral dolostones (FT14), dolostone with evaporite crystals (FT15), bioclastic wackestone to packstone carbonates (FT19), and gypsum-algal beds (FT16) are also intercalated within the gypsiferous marlstones. It originated in shallow seawater, and occasionally in desiccated flooded environments. The regularity and lateral persistence of beds over large areas with only minor changes in thickness, as well as the sudden and episodic occurrence of stromatolite beds and marine bioclastic carbonates, are the main evidence of deposition on broad and very low relief are as affected by rapid marine ingressions and storms, interrupting the more restricted evaporitic conditions with the supply of marine waters during phases of marine influx.

Nowadays similar sediments are depositing in extensive intertidal-supratidal sabkhas (Fig. 14B) settled under arid to semi-arid conditions. Possible modern analogues for such a depositional setting are the coastal sabkhas of the Arabian Gulf, intertidal areas of which are often fully colonized by microbial mats (Alsharhan and Kendall, 2003; Bontognali et al., 2010), the supratidal flats of Florida, and the sabkha flats of the Persian Gulf (Shinn, 1986).

6.2.3. Carbonate system

The carbonate sedimentary system occupies the uppermost Mdaouer Formation and the whole of the Rhoundjaïa Formation. Due to the absence of a slope or a shelf-break evidenced by the absence of re-sedimented low-stand deposits, the wide lateral distribution of facies and the apparent absence of distinct palaeobathymetric changes, the carbonate depositional system represents most likely a low-gradient ramp (homoclinal ramp sensu Burchette and Wright, 1992) (Fig. 14B), represented by four main facies associations (FA4, FA5, FA6 and FA7).

Facies association FA4: inner ramp peritidal to lagoonal carbonates

This facies association constitutes the uppermost part of the Mdaouer Formation and is composed of a thin marlstone interval containing ostracodes (FT11) intercalated between a bioclastic bed rich in bivalves and gastropods (FT19) at the base and a laminated dolomicritic bed (FT13) at the top. This latter displays a wavy and crinkly algal lamination capped occasionally by mud cracks and tepee horizons. Ostracodes evidence marine deposition under low-energy conditions in protected (not restricted) lagoon areas. Algal lamination reflects alternations of sedimentary input and microbial activity and is a common feature in low-energy, microbial-covered, upper intertidal to supratidal settings (Hardie, 1977), confirming deposition in an inner-lagoon/inner shelf environment. Small desiccation cracks and tepee structures all suggest subaerial exposure and shrinking-and-swelling processes characteristic of the supratidal zone (Demicco and Hardie, 1994). The bioclastic limestone bed is interpreted as a marine ingression related to storm events.

Facies association FA5: inner ramp subtidal carbonates

The deposits of this facies association are especially recognizable within the upper part of the lower limestone unit of the Rhoundjaïa Formation. They comprise thick-bedded grey massive limestones with a single bed more than 50 cm thick. The limestone contains a benthic fauna such as ostracodes, benthic foraminifers, pectinid bivalves, oysters, and large gastropods (FT23). Textures are mainly mudstone to wackestone. Bioturbation is represented by rare *Rhizocorallium* and *Planolites* burrows. These deposits indicate high carbonate productivity by dominant benthic organisms. They were most likely formed in a shallow subtidal environment under low energy conditions. The sporadic intercalations of lenticular wackestone–packstone textures, usually rich in oysters (FT20), are suggestive of periodic high energy events (storms).

The inner ramp facies association also covers part of the upper limestone unit, especially in the Rhoundjaïa and Mdaouer sections. It is composed of a bioturbated limestone (FT24) comparable to the Cruziana ichnofacies of Seilacher (1967), suggesting an intertidal to shallow subtidal environment (Bromley, 1967, 1975; Brown and Farrow, 1978).

Facies association FA6: middle ramp carbonates

This facies association is widely expressed in the Rhoundjaïa Formation and combines four predominant facies: high-diversity fauna limestone (FT21), *Neithea*-rich limestone (FT22), massive limestone (FT23) and rudistid limestone (FT25).

In the lower part of the upper limestone unit, throughout the study area, the middle ramp facies association covers a wide range of shallow to relatively deep marine facies including mud-supported fabrics (wackestone to mudstone) with benthic and planktonic fossil assemblages (FT21). The periodic high-energy events (storms) are documented by intercalations of wackestone–packstone texture rich in pectinid genus *Neithea* (FT22). The limestone beds (FT23) containing loose small-patched rudists (FT24) in the Mdaouer section document some patch reefs in a mid-ramp position below the fair-weather wave base with low-energy conditions and open circulation. According to Burchette and Wright (1992), rudist growth within a carbonate mud matrix is a common feature of mid-ramp settings.

Facies association FA7: outer ramp carbonates

This facies association is recorded in the middle marly unit and the upper limestone unit. It consists of highly fossiliferous marlstones (FT12), cephalopod nodular mudstones (FT26), massive limestone devoid of any macrofauna (FT27) and thin-bedded limestone (FT28). The predominant skeletal grains are ammonite, planktonic foraminifers, pelagic crinoids, and calcispheres. Subordinate taxa are smaller benthic foraminifers and tylostomid

gastropods. The microfacies is lime mud-dominated and lacks a shallow-water neritic fauna. No sedimentary features indicative of a shallow-water and high-energy sedimentation have been observed. Large amount of well-preserved pelagic fauna, fine-grained matrix and absence of hydrodynamic structures suggest a permanent low-energy environment probably located below storm wave base (SWB). This facies association is interpreted as deposited in a quieter environment with open circulation related to the outer ramp sub-environment.

7. Sequential evolution

Using the stratigraphic framework and facial changes, as well as the palaeoenvironmental setting and interpretation of outstanding surfaces, the Cenomanian-Turonian succession of the Ksour Mountains can be subdivided into three depositional third-order transgressive–regressive (T–R) sequences that reflect eustatic sea-level changes; within these sequences, maximum flooding surfaces are evidenced by open-marine carbonates.

7.1. Sequence S1

The transgressive half-cycle of the first sequence consists of shoreface deposits of the lower part of the mixed silicoclastic-carbonate unit. Its base is an erosion surface overlain by the first massive carbonate bed of the series. This unconformity, of regional extension, lies at the top of the siliciclastic deposits of the "Continental intercalaire" and corresponds to a transgression surface (Fig. 15). The following regressive half-cycle consists of red and green clays with sandstone and dolomitic levels, of the upper part of the first unit of the El Rhelida Formation. It documents a coastal mud-flat environment. The maximum flooding surface is placed at the top of a sandstone bed displaying wavy cross-bedding and HCS.

7.2. Sequence S2

The transgressive interval of the second sequence corresponds to the deposits of the lower part of the claystone–limestone unit of the El Rhelida Formation. It is linked with the appearance of storm deposits with bioclastic limestone beds, more or less rich in bivalves and gastropods. The maximum flooding surface is placed at the top of a bioclastic carbonate bed with a bioturbated upper surface. The regressive half-cycle of the sequence consists of the coastal deposits of the upper part of the claystone–limestone unit, and of the Mdaouer Formation. Its upper boundary is underlined by an emersion surface with mud-cracks.

7.3. Sequence S3

The third regional transgressive–regressive sequence encompasses the whole Rhoundjaïa Formation. It is of late Cenomanian-early Turonian age. The shallow-water, T–R cycles of the previous sequence (S2) are abruptly overlain everywhere by homogenous mudstones containing a more open-marine fauna (basal part of the lower limestone unit). This lithological change, with peritidal stromatolite limestones passing into mid-ramp pseudo-nodular limestones, can be followed in continuous outcrops all along South Algeria (Benyoucef et al., 2016; Mebarki et al., 2016; Zaoui et al., 2016). This change is interpreted as resulting from a marine opening and deepening. The base of the Rhoundjaïa Formation is thus interpreted as a transgressive surface (Fig. 15). Ammonites found in the uppermost portion of the lower limestone unit, in the middle marly unit, and in the lowermost part of the upper limestone unit are numerous on some bedding planes. Their sudden abundance in the succession suggests a second phase of marine incursion and probable deepening (flooding surface, Fig. 15). Though there is no particular surface suggesting a possible hiatus, the top of the ammonite-bearing limestones is interpreted as a maximum flooding surface (Fig. 15) because the overlying massive limestones are devoid of pelagic fauna, interpreted as of middle ramp environment, and indicative of a shallowing-upward trend (regressive half-cycle).

When using the ammonites as correlation tools, we came to the conclusion that the second half of the transgressive interval covering the uppermost part of the lower limestone unit, the middle marly unit, and the lowermost part of the upper limestone unit, can be correlated with the Late Cretaceous Oceanic Anoxic Event (OAE2); the "BED2" and "BED3" (Grosheny et al., in prep.; S. Ferry, pers. comm.); the second sequence and the transgressive trend of the third sequence deposited in the Southeast Morocco (Lebdel et al., 2012; Lézin et al., 2012; Andreu et al., 2013; Fig. 15, this study). Comparison of the Ksour Mountains and the Tinrhert Basin of Southeast Algeria shows that this latest Cenomanian transgressive interval can be correlated to the upper part of the "Calcaires inférieurs" Formation including the last half of the second unit and most part of the third unit, which cover the $\delta^{13}C$ anomaly (Grosheny et al., 2013; Fig. 15, this study).

The whole Cenomano-Turonian succession is interpreted as a single transgressive–regressive mega-sequence encompassing the different successive sequences, that had been evolving stepwise: from a shore-face environment to an evaporitic flood-plain (or peritidal shelf) interspersed with episodic marine transgressions as evidenced by the bioclastic horizons within green and red claystones/marlstones, and finally to an open-marine (inner-mid-outer shelf) environment as supported by the glut of pelagic and benthic faunas. This mega-sequence corresponds to an epi-cratonic marine transgression over the northern Saharan margin (or South Tethyan margin). It has been thoroughly documented on a greater scale and therefore assumed to be driven by eustasy.

8. Conclusions

The Cenomanian-Turonian succession of the Ksour Mountains has been examined on their stratigraphy, faunal (micro- and macrofauna), ichnologic and sedimentology contents to provide new insights into the palaeo-environment evolution and sea-level changes in southwest Algeria. It has been classified into three lithostratigraphic formations:

The El Rhelida Formation, directly overlying the "Continental intercalaire" group, is assigned to the early Cenomanian age on the basis of vertebrate remains. Its deposits can be related to transgressive silicoclastic shoreface environment vertically passing to coastal mudflat deposits that had been recording several storm events.

The Mdaouer Formation is of early-middle Cenomanian age, from its stratigraphic position and ostracode content. The noteworthy variation in facies characteristics indicates the transition from supratidal, through intertidal to lagoonal conditions, as evidenced by the presence of evaporitic, bioclastic and stromatolitic facies. It is related to an arid climate and a sea level fall.

The Rhoundjaïa Formation is of early late Cenomanian-Turonian age as indicated by ammonites. It is highly fossiliferous and carbonate-dominated, related to the environmental changes caused by the major sea-level transgression. Deposition in the late Cenomanian took place in the middle-ramp area of an open-marine basin. It became deeper during the latest Cenomanian and lower Turonian and passed off in the outer-ramp part of the basin.

The acquired biostratigraphic data document a possible hiatus between the upper Cenomanian and the lower Turonian strata, because upper lower Turonian ammonites (uppermost *Watinoceras coloradoense* Zone) *Pseudotissotia nigeriensis* and *Choffaticeras*

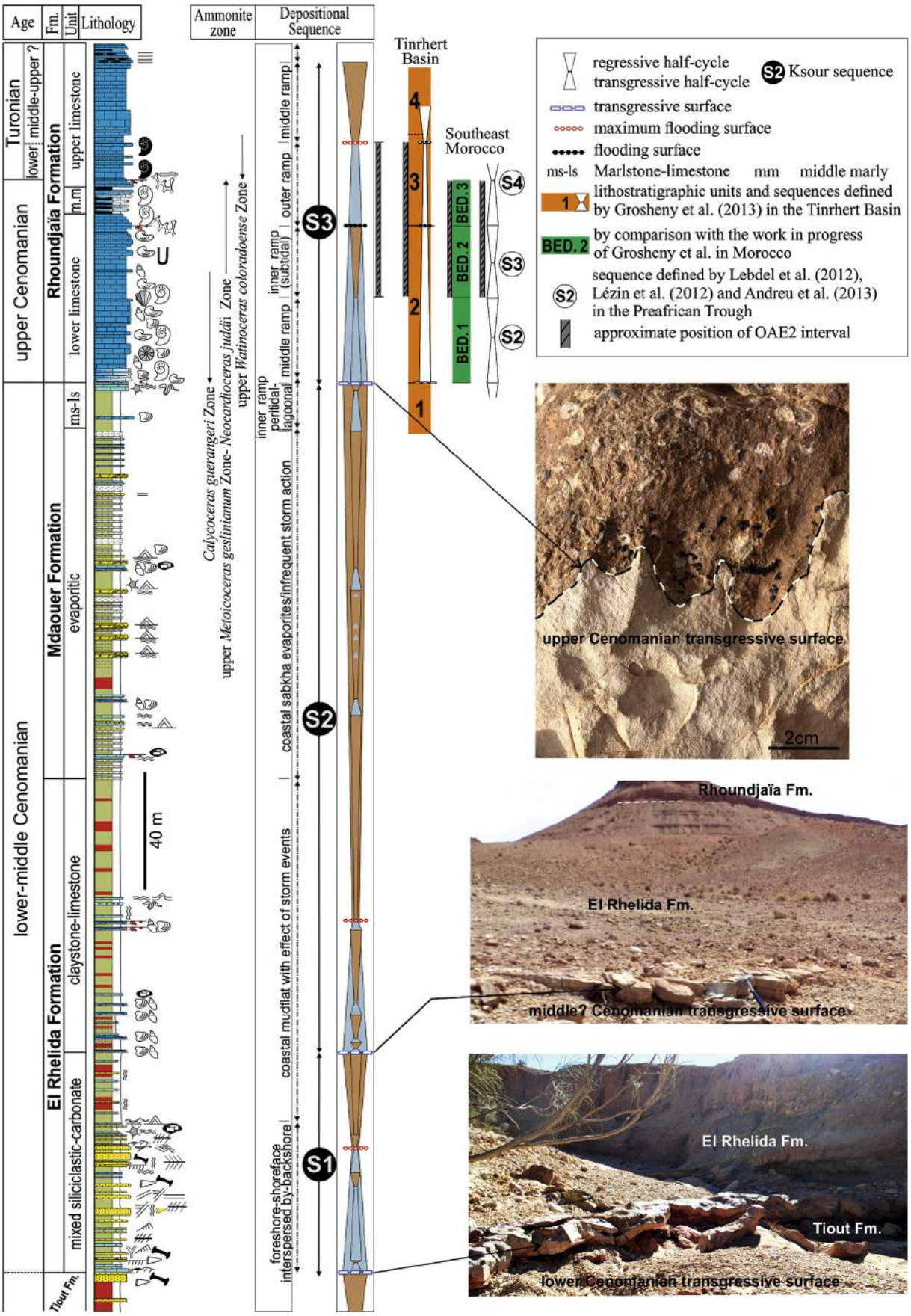

Fig. 15. Sequential organization of the Cenomanian-Turonian strata in the Ksour Mountains.

sinaiticum are directly found overlying the uppermost Cenomanian strata (*Neocardioceras juddii* Zone). This gap is most likely related to a submarine non-deposition.

The extension of depositional areas and the stability of the sedimentary environments were mainly driven by the successive transgressive–regressive fluctuations of the Cenomanian-Turonian sea-level. Identification of depositional sequences is primarily based on the interpretation of facies change, directly reflecting the respective transgressive (deepening-up) and regressive (shallowing-up) system tracts, along with the positioning of some remarkable stratigraphic surfaces (transgressive surface, rapid eustatic fall surface) within observed lithological successions. Weakly-sloped depositional environments may present some incomplete regressive sequences while by-passing some lithological facies usually best-represented in steeper-ramp environments. The identified depositional environments are included into a major framework of three third-order transgressive-regressive sequences (S1, S2, and S3) with sequence boundaries of regional importance. The first two sequences (S1 and S2) assigned to lower-middle Cenomanian consist of the whole deposits of the El Rhelida and Mdaouer formations. The last sequence (S3) attributed to upper Cenomanian-lower Turonian forms the Rhoundjaïa Formation. The whole succession matches well an opening mega-sequence. The general depositional evolution is here related to the eustatic fluctuations during the Cenomanian-Turonian times.

An isotope study as well as our works in progress on both the macro- and micro-fauna of the Cenomanian-Turonian deposits of the Ksour Mountains should complete the present palaeontological record and refine the stratigraphic assignment of the studied succession.

Acknowledgements

The authors are grateful to Danièle Grosheny and to an anonymous reviewer for their critical reviews and constructive suggestions that helped improving the preliminary version of this manuscript. They are also grateful to the Editors of Cretaceous Research, namely Marcin Machalski and Eduardo Koutsoukos, for their highlighting remarks and valuable comments.

References

Aigner, T., 1982. Calcareous tempestites: storm dominated stratification in Upper Muschelkalk limestones (Middle Trias, SW-Germany). 18–198. In: Einsele, G., Seilacher, A. (Eds.), Cyclic and Event Stratification. Springer-Verlag, Berlin.

Aigner, T., Bachmann, G.H., 1989. Dynamic stratigraphy of an evaporite–to–red bed sequence, Gipskeuper (Triassic), south-west German Basin. Sedimentary Geology 62, 5–25.

Alsharhan, A.S., Kendall, C.G.St.C., 2003. Holocene coastal carbonates and evaporites of the southern Arabian Gulf and their ancient analogues. Earth-Science Reviews 61, 191–243.

Ambroggi, R., 1963. Etude géologique du versant méridional du Haut Atlas occidental et de la plaine du Souss. Notes et Mémoires du Service Géologique du Maroc, 157 pp.

Amédro, F., Busson, G., Cornée, A., 1996. Révision des ammonites du Cénomanien supérieur et du Turonien inférieur du Tinrhert (Sahara algérien): implication biostratigraphiques. Bulletin du Muséum national d'Histoire naturelle 18, 179–232.

Andreu, B., Ettachfini, E.M., 1994. Nouvelles espèces du Cénomanien du Bassin d'Essaouira(Maroc). Implications paléoécologiques. Revue de Micropaléontologie 37 (1), 3–29.

Andreu, B., Lebdel, V., Wallez, M.-J., Lézin, C., Ettachfini, El.M., 2013. The upper Cenomanian-lower Turonian carbonate platform of the Preafrican Trough, Morocco: biostratigraphic, paleoecological and paleobiogeographical distribution of ostracods. Cretaceous Research 45, 216–246.

Aref, M., Attiia, O., Wali, A., 1997. Facies and depositional environment of the Holocene evaporites in the Ras Shukeir area, gulf of Suez, Egypt. Sedimentary Geology 110, 123–145.

Bassoullet, J.-P., 1973. Contribution à l'étude stratigraphique du Mésozoïque de l'Atlas Saharien occidental (Algérie). Thèse de Doctorat d'État, Sciences Naturelles. Université de Paris VI, 497 pp.

Bassoullet, J.-P., Damotte, R., 1969. Quelques ostracodes nouveaux du Cénomanien-Turonien de l'Atlas saharien occidental (Algérie). Revue de Micropaléontologie 12 (3), 130–144.

Bauer, J., Kuss, J., Steuber, T., 2003. Sequence architecture and carbonate platform configuration (Late Cenomanian–Santonian), Sinai, Egypt. Sedimentology 50, 387–414.

Benyoucef, M., Meister, C., 2015. Lithostratigraphic evolution, facies analysis and depositional environment of the Cenomanian-lower Turonian in the Guir area, Southwestern Algeria. Cretaceous Research 53, 68–88. http://dx.doi.org/10.1016/j.cretres.2014.10.009.

Benyoucef, M., Adaci, M., Meister, C., Läng, E., Malti, F.-Z., Mebarki, K., Cherif, A., Zaoui, D., Benyoucef, A., Bensalah, M., 2014. Le "Continent intercalaire" dans la région du Guir (Algérie): nouvelles données paléontologiques, ichnologiques et sédimentologiques. Revue de Paléobiologie 33 (1), 281–297.

Benyoucef, M., Läng, E., Cavin, L., Mebarki, K., Adaci, M., Bensalah, M., 2015. Over-abundance of piscivorous dinosaurs (Theropoda: Spinosauridae) in the mid-Cretaceous of North Africa: the Algerian dilemma. Cretaceous Research 55, 44–55. http://dx.doi.org/10.1016/j.cretres.2015.02.002.

Benyoucef, M., Meister, C., Mebarki, K., Läng, E., Adaci, M., Cavin, L., Malti, F.-Z., Zaoui, D., Cherif, A., Bensalah, M., 2016. Evolution lithostratigraphique, paléoenvironnementale et séquentielle du Cénomanien-Turonien inférieur dans la région du Guir (Ouest algérien). Carnets de Geologie 16 (9), 271–295. http://dx.doi.org/10.4267/2042/59926.

Blakey, R.H., 2011. Global Paleogeography. available from website. http://www2.nau.edu/rcb7/65moll.jpg.

Bontognali, T.R.R., Vasconcelos, C., Warthmann, R.J., Bernasconi, S.M., Dupraz, C., Strohmenger, C.J., McKenzie, J.A., 2010. Dolomite formation within microbial mats in the coastal sabkha of Abu Dhabi (United Arab Emirates). Sedimentology 57 (3), 824–844.

Bromley, R.G., 1967. Some observations on burrows of thalassinide an Crustacea in Chalk hardgrounds. Quarterly Journal of the Geological Society of London 123, 157–182.

Bromley, R.G., 1975. Trace fossils at omission surfaces. In: Frey, R.W. (Ed.), The Study of Trace Fossils. Springer-Verlag, New York, pp. 399–428.

Brown, B.J., Farrow, G.E., 1978. Recent dolomitic concretions of crustacean burrow origin from Loch Sunant, west coast of Scotland. Journal of Sedimentary Petrology 48, 825–834.

Buchbinder, B., Ben Jamini, C., Lipson-Benitah, S., 2000. Sequence development of Late Cenomanian-Turonian carbonates ramps, platforms and basins in Israel. Cretaceous Research 21, 813–843.

Burchette, T.P., Wright, V.P., 1992. Carbonate ramp depositional systems. Sedimentary Geology 79, 3–57.

Busson, G., Dhondt, A., Amédro, F., Néraudeau, D., Cornée, A., 1999. La grande transgression du Cénomanien supérieur-Turonien inférieur sur la hamada de Tinrhert (Sahara algérien): datations biostratigraphiques, environnement de dépôt et comparaison d'un témoin épicratonique avec les séries contemporaines à matière organique du Maghreb. Cretaceous Research 20, 29–46.

Cattaneo, A., Steel, R.J., 2003. Transgressive deposits: a review of their variability. Earth-Science Reviews 62, 187–228.

Cavin, L., Tong, H., Boudad, L., Meister, Ch., Piuz, A., Tabouelle, J., Aarab, M., Amiot, R., Buffetaut, E., Dyke, E., Hua, G., Le Loeuff, S.J., 2010. Vertebrate assemblages from the Early Late Cretaceous of Southeastern Morocco: an overview. Journal of African Earth Sciences 57, 391–412.

Chikhi-Aouimeur, F., Grosheny, D., Ferry, S., Herkat, M., Jati, M., Atrops, F., Redjimi-Bourouiba, W., Benkherouf-Kechid, F., 2011. Lithofaciès, paléogéographie et correlations au passage Cénomanien-Turonien dans l'Atlas Saharien (Ouled Naïl, Zibans, Aurès et Hodna, Algérie). Mémoire du Service Géologique de l'Algérie 17, 67–84.

Coffey, B.P., Read, J.F., 2004. Mixed carbonate-siliciclastic sequence stratigraphy of a Paleogene transition zone continental shelf, Southeastern USA. Sedimentary Geology 166, 21–57.

Cornet, A., 1952. L'Atlas saharien Sud-Oranais. Publications du XIXème Congrès Géologique International-Alger, Monographies régionales, 1 ère série, 12 1–51.

Craft, J.H., Bridge, J.S., 1987. Shallow-marine sedimentary processes in the Late Devonian Catskill Sea, New York State. Geological Society of America Bulletin 98, 338–355.

Demicco, R.V., Hardie, L.A., 1994. Sedimentary Structures and Early Diagenetic Features of Shallow Marine Carbonate Deposits. In: SEPM Atlas Series N° 1, 265 pp.

Dewey, J.F., Pitman, W.C., Ryan, W.B.F., Bonnin, J., 1973. Plate tectonics and the evolution of the Alpine system. Geological Society of America Bulletin 84, 3137–3150.

Douihasni, M., 1976. Etude géologique de la région d'Aïn Ouarka –Boussemghoun (partie centrale des Monts des Ksour). Stratigraphie et analyse structurale. Thèse 3ème cycle, Université d'Oran, 2 t., 272 pp., 52 fig., 4 pl.

Einsele, G., Chough, S.K., Shiki, T., 1996. Depositional events and their records – an introduction. Sedimentary Geology 104, 1–9.

Eugster, H.P., Hardie, L.A., 1975. Sedimentation in an ancient playa-lake complex: the Wilkins Peak Member of the Green River Formation of Wyoming. – Geological Society of America Bulletin 86, 319–334. – (1978): Saline Lakes. In: Lerman, A. (Ed.), Chemistry, Geology and Physics of Lakes (p. 237–293). Springer, New York.

Ferré, B., Benyoucef, M., Zaoui, D., Adaci, M., Piuz, A., Tchenar, S., Meister, C., Mebarki, K., Bensalah, M., 2016. Cenomanian-Turonian roveacrinid microfacies assemblages (Crinoidea, Roveacrinida) from the Tinrhert area (SE Algeria). Annales de Paléontologie 102 (4), 225–235. http://dx.doi.org/10.1016/j.annpal.2016.09.001.

Ferré, B., Mebarki, K., Benyoucef, M., Villier, L., Bulot, G.L., Desmares, D., Benachou, H., Marie, L., Sauvagnat, J., Bensalah, M., Zaoui, D., Adaci, M., 2017. Roveacrinids (Crinoidea, Roveacrinida) from the Cenomanian-Turonian of southwest Algeria (Saharan Atlas and Guir Basin). Annales de Paléontologie. http://dx.doi.org/10.1016/j.annpal.2017.03.001.

Flamand, G.B.M., 1911. In: Rey, A. (Ed.), Recherches géologiques et géographiques sur le Haut-Pays de l'Oranie (Algérie et territoire du sud). Thèse ès-Sciences, Lyon, n°47, 1001 pp.

Flügel, E., 2004. Microfacies of Carbonate Rocks, Analysis, Interpretation and Application. Springer-Verlag, Berlin, 976 pp.

Flügel, E., 2010. Microfacies of Carbonate Rocks, Analysis, Interpretation and Application. Springer-Verlag, Berlin, 984 pp.

Galmier, D., 1970. Photogéologie de la région d'Ain Sefra (Algérie). Thèse de Doctorat d'Etat. Faculté des Sciences, Paris, 320 pp.

Geel, T., 2000. Recognition of stratigraphic sequences in carbonate platform and slope deposits: empirical models based on microfacies analysis of paleogene deposits in southeastern Spain. Palaeogeography, Palaeoclimatology, Palaeoecology 155, 211–238.

Ghosh, P., Adkins, J., Affek, H., Balta, B., Guo, W.F., Schauble, E.A., Schrag, D., Eiler, J.M., 2006. 13C-18O bonds in carbonate minerals: a new kind of paleothermometer. Geochimica et Cosmochimica Acta 70, 1439–1456.

Gorican, S., Kosir, A., Rozic, B., Smuc, A., Gale, L., Kukoc, D., Celarc, B., Crne, A.E., Kolarjurkovsek, T., Placer, L., Skaberne, D., 2012. Mesozoic deep-water basins of the eastern Southern Alps (NW Slovenia). In: 29th IAS Meeting of Sedimentology [10-13 September 2012, Schladming]: field trip guides, (Journal of Alpine geology 54). Wien: GEOAUSTRIA 2012, 54, pp. 101–143.

Grosheny, D., Chikhi-Aouimeur, F., Ferry, S., Benkherouf-Kechid, F., Jati, M., Atrops, F., Redjimi-Bourouiba, W., 2008. The Upper Cenomanian-Turonian (Upper Cretaceous) of the Saharan Atlas (Algeria). Bulletin de la Société Géologique de France 179 (6), 593–603.

Grosheny, D., Ferry, S., Jati, M., Ouaja, M., Bensalah, M., Atrops, F., Chikhi-Aouimeur, F., Benkherouf-Kechid, F., Negra, H., Aït Salem, H., 2013. The Cenomanian-Turonian boundary on the Saharan Platform (Tunisia and Algeria). Cretaceous Research 42, 66–84.

Handford, C.R., 1982. Sedimentology and evaporite genesis in a Holocene continental- sabkha playa basin – Bristol Dry Lake, California (USA). Sedimentology 29, 239–253.

Hardie, L.H., 1977. Sedimentation on the Modern Carbonate Tidal Flats of Northwest Andros Island, Bahamas. Johns Hopkins Press, Baltimore, 202 pp.

Harms, J.C., Southard, J.B., Spearing, D.R., Walker, R.G., 1982. Structure and sequence in clastic rocks. Lecture Notes. Society of Economic Paleontologists and Mineralogists, Short Course, 9.

Hofmann, C., Féraud, G., Courtillot, V., 2000. 40Ar/39Ar dating of mineral separates and whole rocks from the western Ghats lava pile: Further constraints on duration and age of the Deccan Traps. Earth and Planetary Science Letters 180, 13–27.

James, N.P., 1979. Shallowing-upward sequences in carbonates, chapter 10. In: Walker, R.G. (Ed.), Facies models: Geoscience Canada Reprint Series 1, pp. 109–119.

Kendall, A.C., 1984. Evaporites. In: Walker, R.G. (Ed.), Facies models, second ed., Geoscience Canada Reprint Series 1, pp. 259–296.

Kennedy, W.J., Walaszczyk, I., Cobban, W.A., 2005. The global boundary stratotype section and point for the base of the Turonian stage of the Cretaceous: Pueblo, Colorado, U.S.A. Episodes 28, 93–104.

Klein, G.V., 1970. Deposition and dispersal dynamics of intertidal sandbars. Journal of Sedimentary Petrology 40, 1095–1127.

Ladipo, K.O., 1986. Tidal shelf depositional model for the Ajali Sandstone, Anambra Basin, Southern Nigeria. Journal of African Earth Sciences 5 (2), 177–185.

Laffite, R., 1939. Etude géologique de l'Aurès. Thèse ès-Sciences, Bulletin du Service de la Carte Géologique de l'Algérie, 2ème série stratigraphie – description régionales 15, 484 pp.

Lamolda, M., Aguado, R., Maurrasse, F.T.-M.R., Peryt, D., 1997. El transito Cretacico–Terciario en Beloc, Haiti: Registro micropaleontologico e implicaciones bioestratigraficas. Geogaceta 22, 97–100.

Lebdel, V., Lézin, C., Andreu, B., Wallez, M.-J., Ettachfini, El M., Riquier, L., 2012. Geochemical and palaeoecological record of the Cenomanian-Turonian Anoxic Event in the carbonate platform of the Preafrican Trough, Morocco. Palaeogeography, Palaeoclimatology, Palaeoecology 369, 79–98.

Lehmann, J., 1999. Integrated stratigraphy and palaeoenvironment of the Cenomanian-Lower Turonian (Upper Cretaceous) of Northern Westphalia, North Germany. Facies 40, 25–70.

Le Loeuff, J., Làng, E., Cavin, L., Buffetaut, E., 2012. Between Tendaguru and Bahariya: on the age of the Early Cretaceous dinosaur sites from the Continental Intercalaire and other African formations. Journal of Stratigraphy 36, 486–502.

Lézin, C., Andreu, B., Ettachfini, ElM., Wallez, M.J., Lebdel, V., Meister, C., 2012. The Upper Cenomanian-Lower Turonian of the Preafrican Trough, Morocco. Sedimentary Geology 245–246, 1–16.

Logan, B.W., 1987. The MacLeod evaporite basin, western Australia. Holocene environments, sediments and geological evolution. American Association of Petroleum Geologists Memoir 44, 1–140.

Mebarki, K., Bulot, L.G., Frau, C., Desmares, D., Villier, L., Benyoucef, M., Adaci, M., Bensalah, M., 2015. Nouvelles données biostratigraphiques sur la limite Cénomanien-Turonien dans les monts des Ksour (Atlas saharien, Ouest de l'Algérie). Annual TOPO-EUROPE workshop, Antibes (France), Oct 4–7, 2015 11–12.

Mebarki, K., Sauvagnat, J., Benyoucef, M., Zaoui, D., Benachour, H.B., Adaci, M., Mahboubi, M., Bensalah, M., 2016. Ostracodes cénomano-turoniens dans l'Atlas saharien occidental et le Bassin du Guir (sud-ouest de l'Algérie) : systématique, biostratigraphie et paléobiogéographie. Revue de Paléobiologie 35 (1), 249–277.

Meister, C., Piuz, A., Cavin, L., Boudad, L., Bacchia, F., Ettachfini, El M., Benyoucef, M., 2017. Late Cretaceous (Cenomanian-Turonian) ammonites from southern Morocco and south western Algeria. Arabian Journal Geosciences 10 (1), 1–46. http://dx.doi.org/10.1007/s12517-016-2714-1.

Miall, A.D., 1985. Architectural-element analysis: a new method of facies analysis applied to fluvial deposits. Earth-Science Reviews 22, 261–308.

Nagm, E., Wilmsen, M., 2012. Late Cenomanian–Turonian (Cretaceous) ammonites from Wadi Qena, central Eastern Desert, Egypt: taxonomy, biostratigraphy and palaeobiogeographic implications. Acta Geologica Polonica 62 (1), 63–89.

Nio, S.D., Yang, C.S., 1991. Sea-level fluctuation and the geometric variability of tide-dominated sand bodies. Sedimentary Geology 70, 161–193.

Paik, I.S., Kim, H.J., 1998. Subaerial lenticular cracks in Cretaceous lacustrine deposits, Korea. Journal of Sedimentary Research 68, 80–87.

Payros, A., Pujalte, V., Tosquella, J., Orue-Etxebarria, X., 2010. The Eocene storm dominated for algal ramp of the western Pyrenees (Urbasa-Andia Formation); an analogue of future shallow-marine carbonate systems. Sedimentary Geology 228, 184–204.

Pettijohn, F.J., Potter, P.E., Siever, R., 1987. Sand and Sandstones. Springer, New York, p. 553.

Reinhardt, L., Ricken, W., 1999. Climate cycles documented in a playa system: comparison of geochemical signatures derived from subbasins (Triassic, Middle Keuper, German Basin). Zentralblatt für Geologie und Paläontologie, Teil I, Geologie 3–4, 315–340.

Schreiber, B.C., Roth, M.S., Helman, M.L., 1982. Recognition of primary facies characteristics of evaporites and the differentiation of these forms from the diagenetic over-prints. In: Handford, C.R., Loucks, R.G., Davies, G.R. (Eds.), Depositional and Diagenetic Spectra of Evaporites: A Core Workshop SEPM Core Workshop 3, pp. 1–32.

Seilacher, A., 1967. Bathymetry of trace fossils. Marine Geology 5, 413–428.

Sereno, P.C., Dutheil, D.B., Iarochene, M., Larsson, H.C.E., Lyon, G.H., Magwene, P.M., Sidor, C.A., Varricchio, D.J., Wilson, J.A., 1996. Predatory Dinosaurs from the Sahara and Late Cretaceous faunal differentiation. Science 272, 986–991.

Shinn, E.A., 1983. Tidal flat environment. In: Scholle, P.A., Bebout, D.G., Moore, C.H. (Eds.), Carbonate Depositional Environments: American Association of Petroleum Geologists Memoir, vol. 33, pp. 172–209.

Shinn, E.A., 1986. Modern carbonate tidal flats: their diagnostic features. Colorado School of Mines Quarterly 81, 7–35.

Spalletti, L., Del Valle A., 1990. Plataformas silicoclasticas, Bossi G., Ambientes y Modelos Sedimentarios Simposio, X Congreso Geológico Argentino, Boletın Sedimentológico 4, 16 pp.

Strasser, A., Pittet, B., Hillgärtner, H., Pasquier, J.B., 1999. Depositional sequences in shallow carbonate-dominated sedimentary systems: concepts for a high-resolution analysis. Sedimentary Geology 128, 201–221.

Stromer, E., 1914. Ergebnisse der Forschungsreisen Prof. E. Stromers in den Wüsten Ägyptens. II. Wirbeltier-Reste der Baharîje-Stufe (unterstes Cenoman). Abhandlungen der Königlich Bayerischen Akademie der Wissenschaften 27, 1–16.

Swift, D.J.P., Niedoroda, A.W., 1985. Fluid and sediment dynamics on continental shelves. In: Tillman, R.W., Swift, D.J.P., Walker, R.G. (Eds.), Shelf Sands and Sandstone Reservoirs, SEPM Short Course Notes 13, pp. 47–133.

Tucker, M.E., Wright, V.P., 1990. Carbonate Sedimentology. Blackwell Scientific Publications, Oxford, 482 pp.

Tunbridge, I.B., 1984. Facies models for a sandy ephemeral stream and clay playa complex; the Middle Devonian Trentishoe Formation of North Devon, UK. Sedimentology 31, 697–716.

Walker, R.G., 1990. Perspective, facies modelling and sequence stratigraphy. Journal of Sedimentary Petrology 60, 777–786.

Walter, S., Herrmann, A.D., Bengtson, P., 2005. Stratigraphy and facies analysis of the Cenomanian–Turonian boundary succession in the Japaratuba area, Sergipe Basin, Brazil. In: Bengtson, P. (Ed.), Mesozoic palaeontology and stratigraphy of South America and the South Atlantic, Part II, Journal of South American Earth Sciences, 19(3), pp. 273–283.

Warren, J.W., 1982. The hydrological setting, occurrence and significance of gypsum in Late Quaternary salt lakes in south Australia. Sedimentology 29, 609–637.

Wilson, J.L., 1975. Carbonate Facies in Geologic History. Springer Verlag, Berlin Heidelberg New York, 470 pp.

Wilson, M., Evans, M.J., 2002. Sedimentology and diagenesis of Tertiary carbonates on the Mangkalihat Peninsula, Borneo: implications for subsurface reservoir quality. Marine and Petroleum Geology 19 (7), 873–900.

Zaoui, D., Tchenar, S., Benyoucef, M., Meister, C., Adaci, M., Piuz, A., Mebarki, K., Bensalah, M., Gabani, A., Mahboubi, M., 2016. Le Cénomano-Turonien dans la Hamada du Tinrhert (Sahara, Algérie): résultats préliminaires. Revue de Paléobiologie 35 (2), 541–559.